SENSITIVITY ANALYSIS OF GROUND-WATER MODELS

by

Carl D. McElwee

Kansas Geological Survey
The University of Kansas
Lawrence, Kansas 66046

Prepared for presentation at the
NATO Advanced Study Institute on
Fundamentals of Transport Phenomena in Porous Media

Kansas Geological Survey
Open File Report 85-9
June, 1985

SENSITIVITY ANALYSIS OF GROUND WATER MODELS

1. Introduction.

   One goal of this paper is to develop a better understanding of model insensitivity.

   Another goal is to outline a general sensitivity analysis formalism.

   The sensitivity analysis formalism will be illustrated by application to a number of simple models.

   The final goal is to develop some general guidelines for designing models that have the desired sensitivity to model parameters.

2. General Definition of Sensitivity Coefficients.

   2.1 Models with constant parameters.

   2.2 Models with spatially varying parameters.

   2.3 General comments about sensitivity coefficients.

3. Methods for Determining Sensitivity Coefficients.

   3.1 Analytical expressions for the sensitivity coefficients.

   3.2 Finite difference expression for sensitivity coefficients.

   3.3 A partial differential equation for sensitivity coefficients.

4. Examples of Sensitivity Coefficients.

   4.1 The Theis equation.

   4.2 The Hantush radial leaky aquifer.

   4.3 One-dimensional model with spatially varying transmissivity.

   4.4 A simple two-dimensional model with spatially varying transmissivity.

5. Effect of Boundary Conditions on Sensitivity Coefficients.

   5.1 Finite radial confined aquifer.

   5.2 Alternate boundary conditions for the one-dimensional aquifer.

   5.3 Alternate boundary conditions for the simple two-dimensional model.

6. The Role of Sensitivity Coefficients in Parameter Estimation.

    6.1 Ordinary least squares.

    6.2 Other methods.

7. Using Sensitivity Coefficients to Estimate Confidence Regions.

    7.1 Confidence intervals and regions for estimated parameters.

    7.2 Confidence intervals for calculated head.

8. Model Design for Maximum Sensitivity.

    8.1 Minimize the estimated errors or confidence intervals.

        Consider the effects of measurement locations and times, parameter dependence and correlation, boundary conditions, and parameter zonation.

    8.2 Examples of methods of maximizing model sensitivity.

        8.2.1 The Theis aquifer.

        8.2.2 The leaky aquifer.

        8.2.3 One-dimensional steady-state model with spatially varying transmissivity.

        8.2.4 One-dimensional transient model with spatially varying parameters.

        8.2.5 Two-dimensional steady-state models.

9. Summary and Conclusions.

    The goal is to select a model with maximum sensitivity to the aquifer parameters based on a knowledge of sensitivity coefficients and their properties.

SENSITIVITY ANALYSIS OF GROUND-WATER MODELS

Carl D. McElwee

Kansas Geological Survey
The University of Kansas
1930 Constant Avenue
Lawrence, Kansas, 66046, U.S.A.

ABSTRACT

One of the most difficult tasks in ground-water modeling is the estimation of aquifer parameters from field measurements of hydraulic head. This paper examines model sensitivity through the use of sensitivity analysis. For each model parameter one can define a sensitivity coefficient. These sensitivity coefficients depend on the choice of model, the spatial coordinates, the time variable, the number and type of model parameters, and the boundary conditions. For good sensitivity to the parameters, all sensitivity coefficients should be independent and as large as possible at the locations and times of interest. Methods for determining sensitivity coefficients are discussed and some typical examples showing certain important characteristics are presented. The sensitivity coefficients can be used to estimate variances and confidence intervals for the aquifer parameters. The model sensitivity can be increased for parameter estimation by applying some general principles from sensitivity analysis. Several examples of improved sensitivity are presented.

1. INTRODUCTION

One of the most difficult tasks in ground-water modeling involves estimation of the aquifer parameters to be used in a predictive ground-water model. Usually some historical hydraulic head data are available along with some field or laboratory estimates of the aquifer parameters. These data are usually sparse and of varying quality. Estimation of the aquifer parameters from hydraulic head data is generally recognized to be difficult and may be unstable or nonunique [Yakowitz and Duckstein (19)]. One goal of this paper is to develop a better understanding of model sensitivity to the

aquifer parameters.

Sensitivity analysis is the primary tool used to investigate parameter estimation in this paper. A general first-order sensitivity analysis formalism is presented to calculate the perturbed head caused by a change in an aquifer parameter. A central figure in the formalism is the sensitivity coefficient. When the sensitivity coefficients are known, the parameter variances can be calculated. A large parameter variance means the model is not very sensitive to that parameter. Therefore, some time is devoted to methods for determining sensitivity coefficients. The sensitivity coefficients are affected by the choice of model, the number and type of parameters, and the boundary conditions. In addition, the sensitivity coefficients are functions of space and time. Several examples of sensitivity coefficients for a variety of models and boundary conditions are presented.

The final goal of this paper is to develop some general principles or guidelines for designing models that have the desired sensitivity to model parameters. This is done by looking in detail at how the sensitivity coefficients enter the least squares estimation procedure and how the sensitivity coefficients are affected by the model specification. The model specification includes such things as the model equations, the boundary conditions, and the number of parameters or parameter zones. In general, one might suppose it is desirable to make the sensitivity coefficients as large as possible. Also, it might be that the chosen parameters should be independent. In section 8 these questions are dealt with in more detail and some general conclusions are stated. Several examples of improved sensitivity, obtained by applying the guidelines, are also presented in section 8.

2. GENERAL DEFINITION OF SENSITIVITY COEFFICIENTS

When a model is used to describe the hydraulic head distribution (h) in a ground-water system, the head is assumed to depend uniquely upon the physical parameters input to the model.

$$h = h[\underline{x},t;T(\underline{x}),S(\underline{x}),Q(\underline{x},t)] \qquad (2.1)$$

T, S, and Q are respectively transmissivity, storativity, and flux of water in or out of the system. $\underline{x}$ is a vector containing the appropriate number of coordinates for the model dimensionality (usually one or two). It has been assumed that the transmissivity and storativity do not depend upon time (t). This assumption means that unconfined aquifers and delayed yield will not be explicitly considered. In this work $Q(\underline{x},t)$ will be assumed to be known. Only the variation of the model response to changes in $T(\underline{x})$ and $S(\underline{x})$ will

be considered.

In studying the sensitivity of a ground-water-flow system to parameter variations, a mathematical model must be specified:

$$F[\underline{x},t,h;T(\underline{x}),S(\underline{x}),Q(\underline{x},t)] = 0. \tag{2.2}$$

The model specification represented symbolically by F in Eq. (2.2) includes such things as initial conditions, boundary conditions, and the appropriate differential equations. Eq. (2.2) may be solved analytically or numerically.

2.1 Models with Constant Parameters

For models with constant parameters, the solution to (2.2) can be written as

$$h = h(\underline{x},t;T,S,Q). \tag{2.3}$$

Consider the variation of one of the parameters, T, for example. Eq. (2.2) now becomes

$$F(\underline{x},t,h^*;T+\Delta T,S,Q) = 0 \tag{2.4}$$

where h* is the perturbed head. Solution of (2.4) gives

$$h^* = h^*(\underline{x},t;T+\Delta T,S,Q). \tag{2.5}$$

The sensitivity coefficient for variations in T is defined as

$$U_T(\underline{x},t;T,S,Q) = \frac{\partial h}{\partial T} = \lim_{\Delta T \to 0} \frac{\Delta h}{\Delta T}, \tag{2.6}$$

where $\Delta h = h^* - h$.

A similar development for the storage coefficient allows the two sensitivity coefficients to be written as

$$U_T(x,t) = \frac{\partial h(x,t;T,S,Q)}{\partial T} \tag{2.7}$$

$$U_S(x,t) = \frac{\partial h(x,t;T,S,Q)}{\partial S} \, . \tag{2.8}$$

The functional dependence on T, S, and Q has been dropped on the left-hand side of Eqs. (2.7) and (2.8) for convenience in writing U_T and U_S. However, the sensitivity coefficients do depend on T, S, Q, the initial conditions, the boundary conditions, and the underlying model Equations.

The solution of the flow equation (2.4) is assumed to depend analytically upon the parameters T and S, and T, S, and Q are independent of each other. Now consider a perturbation of the transmissivity, ΔT . Since it has been assumed that the solutions depend analytically on the parameters, the function $h^*(\underline{x},t;T+\Delta T,S,Q)$ may be expanded into a Taylor series. If ΔT is small, the second- and higher-order terms may be neglected.

$$h^*(\underline{x},t;T+\Delta T,S,Q) \simeq h(\underline{x},t;T,S,Q) + U_T \Delta T \tag{2.9}$$

Thus the new head produced by a perturbation in transmissivity (ΔT) may be calculated from (2.9) if the sensitivity coefficient and the unperturbed head are known. Similarly, if a perturbation in storage coefficient (ΔS) occurs, the perturbed head is given by

$$h^*(x,y,t;T,S+\Delta S,Q) \simeq h(x,y,t;T,S,Q) + U_S \Delta S \tag{2.10}$$

to first order in ΔS .

Eqs. (2.7) and (2.8) show that it would be desirable to calculate U_T and U_S for a given model, if possible. Then the response of the model to various perturbations could be calculated simply from (2.7) or (2.8) without actually evaluating the model equations again. The work of McElwee and Yukler (11) indicates that Eqs. (2.9) and (2.10) should be valid for parameter variations of about 20% or less.

2.2 Models With Spatially Varying Parameters

In the more general case where transmissivity and storativity vary with space, a slightly different procedure is used to define the sensitivity coefficients. h will be the hydraulic head resulting from a transmissivity distribution $T(\underline{x})$. Let h^* represent the

hydraulic head that results when the transmissivity distribution is changed at one point ($\underline{x}_o$) by a small amount $\Delta T(\underline{x}_o)$.

$$\frac{\Delta h(\underline{x},t;\underline{x}_o)}{\Delta T(\underline{x}_o)} = [h^*(\underline{x},t;T(\underline{x})+\delta(\underline{x}-\underline{x}_o)\Delta T(\underline{x}_o),S(\underline{x}),Q(\underline{x},t)) - h(\underline{x},t;T(\underline{x}),S(\underline{x}),Q(\underline{x},t))]/\Delta T(\underline{x}_o) \qquad (2.11)$$

The symbol $\delta(\underline{x}-\underline{x}_o)$ represents the Dirac delta function [Lighthill (10)]. x is assumed to be a unitless variable so that $\delta(\underline{x}-\underline{x}_o)$ is also unitless. The sensitivity with respect to variations in transmissivity is defined as

$$U_T(\underline{x},t;\underline{x}_o) = \lim_{\Delta T(\underline{x}_o)\to 0} \frac{\Delta h(\underline{x},t;\underline{x}_o)}{\Delta T(\underline{x}_o)} . \qquad (2.12)$$

This sensitivity coefficient tells how much the head will be changed at point $\underline{x}$ due to a change in transmissivity $\Delta T(\underline{x}_o)$ at point $\underline{x}_o$. Since $\Delta T(\underline{x}_o)$ is assumed to be small, a first-order expansion may be employed to obtain

$$h^* \simeq h + U_T(\underline{x},t;\underline{x}_o)\Delta T(\underline{x}_o). \qquad (2.13)$$

If the transmissivity is changed at more than one point, then the change in head Δh must be found by integrating over the area (or volume), A (or V), where $T(\underline{x})$ is changed

$$h^* - h = \Delta h(\underline{x},t) = \int_A U_T(\underline{x},t;\underline{x}_o)\Delta T(\underline{x}_o)d\underline{x}_o. \qquad (2.14)$$

Outside the region A (or V), $\Delta T(x_o)$ is zero. In the special case when the transmissivity is to be changed by a constant amount ΔT everywhere, Eq. (2.14) becomes

$$h^* - h = \Delta h(\underline{x},t) = \Delta T \cdot U_T(\underline{x},t) \qquad (2.15)$$

where

$$U_T(\underline{x},t) = \int_A U_T(\underline{x},t;\underline{x}_o)d\underline{x}_o . \qquad (2.16)$$

In the preceding development, $\underline{x}$ and $\underline{x}_o$ are assumed to be appropriate dimensionless variables.

A similar development for the sensitivity with respect to storativity (U_S) yields

$$h^* - h = \Delta h(\underline{x},t) = \int_A U_S(\underline{x},t;\underline{x}_o)\Delta S(\underline{x}_o)d\underline{x}_o \tag{2.17}$$

and

$$h^* - h = \Delta h(x,t) = \Delta S \int_A U_S(\underline{x},t;\underline{x}_o)d\underline{x}_o = \Delta S \cdot U_S(\underline{x},t) \tag{2.18}$$

when ΔS is constant over the region of integration. As before,

$$U_S(\underline{x},t;\underline{x}_o) = \lim_{\Delta S(\underline{x}_o)\to 0} \frac{\Delta h(\underline{x},t;\underline{x}_o)}{\Delta S(\underline{x}_o)} \tag{2.19}$$

where

$$\Delta h(\underline{x},t;\underline{x}_o) = h^*(\underline{x},t;T(\underline{x}),S(\underline{x})+\delta(\underline{x}-\underline{x}_o)\Delta S(\underline{x}_o),Q(\underline{x},t)) - h(\underline{x},t;T(\underline{x}),S(\underline{x}),Q(\underline{x},t)). \tag{2.20}$$

The sensitivity coefficients U_T and U_S are seen to be the quantities needed to calculate the response of a model to perturbations in the spatial distribution of transmissivity and storage. Consequently, a discussion of some of the general properties of sensitivity coefficients is in order. In later sections, procedures for determining sensitivity coefficients will be illustrated.

2.3 General Comments About Sensitivity Coefficients

The sensitivity coefficients will depend on the independent variables (space and time), the model parameters (T, S, etc.), and the boundary conditions. Each of these factors may have a dramatic effect on the model sensitivity and thus on any attempt to perform inverse calculations. Much of this paper will be concerned with studying these effects. The general confined flow equation can be written for some region (R, Figure 1) as

$$\frac{\partial}{\partial \underline{x}}\left[\frac{T(\underline{x})}{T_{max}}\frac{\partial h}{\partial \underline{x}}\right] = \left[\frac{S_{max}}{T_{max}}\right]\left[\frac{S(\underline{x})}{S_{max}}\right]\frac{\partial h}{\partial t} - \frac{Q'(\underline{x},t)}{T_{max}} \tag{2.21}$$

where T_{max} and S_{max} are the maximum values of the transmissivity and

storativity, respectively. Q' is the specified water flux per unit area of the model (Q/A) and would be caused by pumpage, injection, leakage, etc. In addition to the flow equation, we need boundary and initial conditions for a complete solution to the hydraulic head and the sensitivity coefficients. Typical boundary conditions are head specified

$$h = H \text{ on } \Gamma_1 \tag{2.22}$$

and flux specified

$$Q''(\Gamma_2,t) = - T\left[\frac{\partial h}{\partial n}\right]_{\Gamma_2} \text{ on } \Gamma_2. \tag{2.23}$$

Γ is the boundary ($\Gamma = \Gamma_1 + \Gamma_2$) of region R (Figure 1). Q" is the specified flux per unit length (Q/ℓ) of boundary Γ_2. The initial condition can be specified as

$$h(\underline{x},0) = f(\underline{x}) \text{ in } R\ . \tag{2.24}$$

Eqs. (2.21) through (2.24) illustrate how the head and, consequently, the sensitivity coefficients depend upon the transmissivity and storativity. The head can be written symbolically as

$$h = h\left[\underline{x}, \frac{T_{max}}{S_{max}} t; \frac{T(\underline{x})}{T_{max}}, \frac{S(\underline{x})}{S_{max}}, \frac{Q(\underline{x})}{T_{max}}\right] \tag{2.25}$$

provided Q and the boundary conditions do not depend upon time. If Q and the boundary conditions do depend upon time, then additional time dependence besides $[(T_{max}/S_{max})t]$ may be introduced in the head solution. $T(\underline{x})/T_{max}$ and $S(\underline{x})/S_{max}$ represent normalized distributions for the transmissivity and storativity which vary between the limits of zero and one. They specify the shape of the T and S variation, but not the absolute magnitudes.

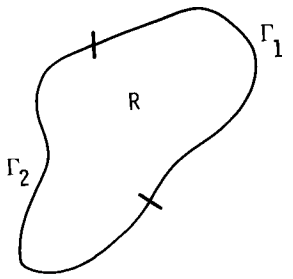

Fig. 1. Region of solution and boundaries for a model.

Next, a few simple observations are made regarding sensitivity coefficients. At steady state ($\partial h/\partial t = 0$), h does

not depend on $S(\underline{x})$. Therefore, U_S is zero at steady state and is small as one nears steady state. In the homogeneous case $T(\underline{x}) = T_{max}$ and $S(\underline{x}) = S_{max}$ and Eq. (2.25) reduces to

$$h = h(\underline{x}, \frac{T}{S} t) \tag{2.26}$$

when the specified fluxes, $Q(\underline{x})$, are zero. If all specified fluxes are zero, only barrier or specified head boundaries are used. From Eqs. (2.26), (2.7), and (2.8), the sensitivity coefficients U_T and U_S can be shown to be dependent:

$$U_T = - \frac{S}{T} U_S. \tag{2.27}$$

This means that the inverse problem is nonunique since any value of S and T with the correct ratio will give a good solution.

Even if one allows spatial variation in T and S in Eq. (2.25), the inverse problem is still nonunique since any S_{max} and T_{max} having the same ratio will give an equally good solution provided there are no specified fluxes in the model. Theoretically, a specified T on each streamline will uniquely determine the transmissivity distribution and, consequently, the storativity distribution. Some inverse procedures [Knowles et al. (9)] solve for the fluxes, Q, in addition to the transmissivity and storativity. The foregoing discussion and Eq. (2.25) show that, when both Q and T are adjusted, an additional level of nonuniqueness is introduced since only the ratios of Q and T need to be held constant. In others words, Q and T are not independent parameters.

Some initial condition must be specified for the hydraulic head at the beginning of a model simulation; consequently, this condition determines the initial condition on the sensitivity coefficients. The sensitivity coefficients may or may not start out zero. One commonly used initial condition is a flat head distribution. In this case, the sensitivity coefficients (U_T and U_S) have an initial value of zero. Another commonly used initial condition is a steady-state head distribution. (Additional fluxes, $Q(\underline{x})$, are imposed and future changes are predicted.) For a steady-state initial condition, U_S is zero, but U_T will not in general be zero. The initial values of U_T may be found by solution of equations to be discussed later.

When the sensitivity coefficients are zero or not independent, the inverse process will not work. This result is inherent in the model and does not depend on the details of the inverse process. In actual practice, the inverse process may experience difficulty when

the sensitivity coefficients are very small but not zero. In this case, the model is simply not very sensitive to changes in aquifer parameters. By calculating and examining the sensitivity coefficients, one may obtain an indication of the stability of the inverse process. As a rule-of-thumb, the sensitivity coefficients should be as large as possible and be independent for a stable inverse problem.

3. METHODS FOR DETERMINING SENSITIVITY COEFFICIENTS

In this section various methods for determining sensitivity coefficients are considered. Three methods will be considered: analytical expressions, finite difference approximations, and solution of a partial differential equation.

3.1 Analytical Expressions For The Sensitivity Coefficients

Sometimes analytical formulas for the head or drawdown can be found for simple models. In many of these cases, finding convenient analytical expressions for the sensitivity coefficients is also possible. As an example, consider the Theis equation. The Theis equation [Theis (18)] describes radial confined ground-water flow in a uniformly thick, horizontal, homogeneous, isotropic aquifer of infinite areal extent.

$$s = \frac{Q}{4\pi T} \int_{(r^2 S/4Tt)}^{\infty} \frac{e^{-u}}{u}\, du \qquad (3.1)$$

In the above equation s is drawdown (L), Q is the discharge (L^3/T), T is the transmissivity (L^2/T) , t is the time (T), S is the dimensionless storage coefficient, and r is the radial observation distance from the pumped well (L).

The sensitivity coefficients may be obtained from Eq. (3.1) by applying the definitions given in equations (2.7) and (2.8). After applying Leibnitz's rule for differentiating an integral [Hildebrand (8)] to Eq. (3.1), one obtains [McElwee and Yukler (11)]

$$U_S = \frac{\partial s}{\partial S} = - \frac{Q}{4\pi TS} \exp(- \frac{r^2 S}{4Tt}) \qquad (3.2)$$

and

$$U_T = \frac{\partial s}{\partial T} = - \frac{s}{T} - \frac{S}{T} U_s \qquad (3.3)$$

These equations for the sensitivity coefficients may be evaluated quite easily if one can evaluate the drawdown (s). Notice that, if

not for the first term on the right of Eq. (3.3), U_T and U_S would be dependent. Eqs. (3.2) and (3.3) will be discussed and plotted in a later section of this paper.

As a further example, consider the leaky confined aquifer. The aquifer system, defined by Hantush and Jacob (7), is composed of a level, isotropic, homogeneous, porous medium of infinite areal extent. The lower aquifer boundary is assumed to be impervious, while the upper boundary is assumed to be a leaky confining bed. Water is derived from the aquifer by elastic expansion of the water and compression of the aquifer matrix as pumping occurs. Leakage through the semiconfining bed is assumed to be proportional to the drawdown in the semiconfined aquifer. It is assumed that no water is removed from storage in the semiconfining unit and that no drawdown occurs in the source bed. The analytical solution for the drawdown is

$$s = \frac{Q}{4\pi T} \int_u^\infty \frac{1}{y} \exp\left(-y - \frac{L^2 r^2}{4y}\right) dy, \tag{3.4}$$

$$u = r^2 S/4Tt, \quad L^2 = K'/Tm'$$

where K' is the permeability of the semiconfining bed, m' is the thickness of the semiconfining bed, and the other quantities are the same as for the Theis equation. By applying Leibnitz's rule for differentiating an integral [Hildebrand (8)], obtaining the sensitivity coefficients with respect to S and T is easy [Cobb, McElwee, and Butt (2)]:

$$U_S = \frac{\partial s}{\partial S} = - \frac{Qr^2}{16\pi T^2 t} \left[\frac{1}{u} \exp\left(-u - \frac{L^2 r^2}{4u}\right)\right] \tag{3.5}$$

$$U_T = \frac{\partial s}{\partial T} = - \frac{s}{T} - \frac{S}{T} U_S. \tag{3.6}$$

As before, these expressions are easy to evaluate if the drawdown has been calculated previously.

These two examples of analytical expressions for the sensitivity coefficients are typical. Many more examples could be presented for simple models.

3.2 Finite Difference Expression For Sensitivity Coefficients

Sometimes it is not convenient or possible to come up with an

analytical formula to be evaluated for the sensitivity coefficients. In these cases, one can always evaluate the sensitivity coefficients numerically by a finite difference approximation if the head or drawdown can be calculated. To illustrate this process, we continue with the leaky confined aquifer of the previous section. If we try to evaluate U_L, the sensitivity with respect to leakage, by differentiating Eq. (3.4), we obtain [Cobb, McElwee, and Butt (2)]

$$U_L = \int_u^\infty \{-Lr^2/2y^2\} \exp(-y - L^2r^2/4y)\, dy. \tag{3.7}$$

Note that both U_S and U_T in Eqs. (3.5) and (3.6) can be expressed in such a manner that, after the drawdown (s) is computed, no further numerical integration is required. The sensitivity with respect to leakage, U_L in Eq. (3.7), can be computed only by additional numerical integration that would involve the formulation of a more complex subroutine. Therefore, the decision might be made to generate U_L by a finite difference approximation. The approximation

$$U_L = \partial s/\partial L \simeq \{s(L+\Delta L) - s(L-\Delta L)\}\ /2\Delta L \tag{3.8}$$

becomes increasingly accurate as ΔL approaches zero. Satisfactory evaluation of U_L occurred for ΔL set equal to .01 L. Plots of U_L will be presented later. This or a similar finite difference scheme could be used to calculate the sensitivity coefficients in many situations.

3.3 A Partial Differential Equation For Sensitivity Coefficients

For the general time-dependent case when transmissivity and storativity can vary spatially, no closed-form expression exists for the head and the sensitivity coefficients. The head is given by the solution of the following partial differential equation [or equivalently Eq. (2.21)].

$$\frac{\partial}{\partial \underline{x}} \left[T(\underline{x}) \frac{\partial h}{\partial \underline{x}}\right] = S(\underline{x}) \frac{\partial h}{\partial t} - Q'(\underline{x},t) \tag{3.9}$$

A partial differential equation for the sensitivity with respect to transmissivity can be developed by applying some of the definitions given earlier. If h* is the new head that results when the transmissivity is changed by $\Delta T(\underline{x}_o)$ at $\underline{x}_o$, then

$$\frac{\partial}{\partial \underline{x}}\left[T(\underline{x})\,\frac{\partial h^*}{\partial \underline{x}}\right] + \frac{\partial}{\partial \underline{x}}\left[\delta(\underline{x}-\underline{x}_o)\,\Delta T(\underline{x}_o)\,\frac{\partial h^*}{\partial \underline{x}}\right] =$$

$$S(\underline{x})\,\frac{\partial h^*}{\partial t} - Q'(\underline{x},t). \qquad (3.10)$$

Applying the definition of $U_T(\underline{x},t;\underline{x}_o)$, Eq. (2.12) results in the following expression.

$$\frac{\partial}{\partial \underline{x}}\left[T(\underline{x})\,\frac{\partial U_T(\underline{x},t;\underline{x}_o)}{\partial \underline{x}}\right] + \frac{\partial}{\partial \underline{x}}\left[\delta(\underline{x}-\underline{x}_o)\,\frac{\partial h}{\partial \underline{x}}\right] =$$

$$S(\underline{x})\,\frac{\partial U_T(\underline{x},t;\underline{x}_o)}{\partial t} \qquad (3.11)$$

In deriving Eq. (3.11), Eq. (3.9) has been subtracted from Eq. (3.10), the result divided by $\Delta T(\underline{x}_o)$, and the limit taken as $\Delta T(\underline{x}_o)\to 0$.

Eq. (3.11) is a partial differential equation for $U_T(\underline{x},t;\underline{x}_o)$ which looks very much like the original flow equation except for two differences. First, the fluxes $[Q(\underline{x})]$ do not appear in Eq. (3.11). Second, there is an additional term involving the differentiation of a delta function.

Except in very simple cases, numerical methods must be used to solve Eq. (3.9). The question arises as to how equation (3.11) may be used with numerical methods to obtain $U_T\ (\underline{x},t;\underline{x}_o)$. Only the term involving the differentiation of the delta function will be considered. The other terms in Eq. (3.11) are similar to terms in the flow Eq. (3.9) and may be handled with standard techniques. The elementary central difference formula for the partial derivative in the x direction of an arbitrary function f(x,y) evaluated at point (x_i,y_j) is

$$\left[\frac{\partial f(x,y)}{\partial x}\right]_{\substack{x=x_i\\ y=y_j}} \simeq \frac{f_{i+1/2,j} - f_{i-1/2,j}}{\Delta x} \qquad (3.12)$$

where a uniformly spaced node system is assumed such that $x_i = i\Delta x$ and $y_j = j\Delta y$. At this point let the grid system for specifying T to be arbitrary and simply denote the value of T at some point $\underline{x}_o(x_k y_\ell)$ by $T_{k,\ell}$. The x component of the delta function term in Eq. (3.11) is

$$\frac{\partial}{\partial x}\left[\delta(x-y_k)\delta(y-y_\ell)\frac{\partial h}{\partial x}\right]_{\substack{x=x_i\\y=y_j}} \simeq \frac{\delta_{j,\ell}}{\Delta x^2}\left[\delta_{i+1/2,k}\cdot\right.$$

$$\left.(h_{i+1,j}-h_{i,j})-\delta_{i-1/2,k}(h_{i,j}-h_{i-1,j})\right] \qquad (3.13)$$

where $\delta_{i,j}$ is the Kronecker delta with the following properties

$$\delta_{i,j}=\begin{cases}1 \text{ if } i=j\\ 0 \text{ if } i\neq j\end{cases} \qquad (3.14)$$

Notice that specifying the transmissivity half way between the nodes where h is known is convenient. Eq. (3.13) gives the finite difference numerical approximation of the delta function term in Eq. (3.11). An alternate procedure could be performed for a finite element approximation.

Usually Eq. (3.11) would not be solved for point changes in the transmissivity. Rather, the transmissivity is usually assumed to be constant over a zone which includes several points or nodes. According to Eq. (2.16) we must integrate Eq. (3.11) over that zone to obtain the sensitivity with respect to transmissivity in that zone. This would be equivalent to summing Eq. (3.13) over all k and ℓ values in that zone.

$$\int_{\substack{\text{zone}\\ m}}\frac{\partial}{\partial x}\left[\delta(x-x_k)\delta(y-y_\ell)\frac{\partial h}{\partial x}\right]_{\substack{x=x_i\\y=y_j}}dA \simeq \sum_{\substack{k,\ell\\ \text{zone}\\ m}}\frac{\delta_{j,\ell}}{\Delta x^2}\cdot$$

$$\left[\delta_{i+1/2,k}(h_{i+1,j}-h_{i,j})-\delta_{i-1/2,k}(h_{i,j}-h_{i-1,j})\right] \qquad (3.15)$$

The partial differential equation for the sensitivity with respect to storativity is somewhat easier to obtain. If h* is the new head that results when the storativity is changed by $\Delta S(\underline{x}_o)$ at $\underline{x}_o$ then

$$\frac{\partial}{\partial \underline{x}}\left[T(\underline{x})\frac{\partial h^*}{\partial \underline{x}}\right]=\left[S(\underline{x})+\delta(\underline{x}-\underline{x}_o)\Delta S(\underline{x}_o)\right]\frac{\delta h^*}{\delta t}-Q'(\underline{x},t). \qquad (3.16)$$

Subtracting Eq. (3.9) from Eq. (3.16), dividing by $\Delta S(\underline{x}_o)$, and taking the limit as $\Delta S(\underline{x}_o)\to 0$ results in the following equation.

$$\frac{\partial}{\partial \underline{x}}\left[T(\underline{x})\,\frac{\partial U_S(\underline{x},t;\underline{x}_o)}{\partial \underline{x}}\right] = S(\underline{x})\,\frac{\partial U_S(\underline{x},t;\underline{x}_o)}{\partial t} + \delta(\underline{x}-\underline{x}_o)\,\frac{\delta h}{\delta t} \quad (3.17)$$

Recall that the definition of U_S is given by Eq. (2.19).

Once again, Eq. (3.17) looks identical in form to the flow equation except there are no fluxes [Q(x)] and the delta function term has been added. The finite difference numerical solution of Eq. (3.17) is carried out in a manner similar to that used for the flow equation except for the delta function term. If Eq. (3.17) is to be evaluated at $\underline{x} = (x_i, y_j)$ and $\underline{x}_o = (x_k, y_\ell)$ then

$$\left[\delta(x-x_k)\delta(y-y_\ell)\,\frac{\delta h}{\delta t}\right]^{n+1/2}_{\substack{x=x_i \\ y=y_j}} \simeq \frac{(h^{n+1}_{i,j} - h^{n}_{i,j})}{\Delta t}\,\delta_{i,k}\delta_{j,\ell} \quad (3.18)$$

where Δt is the time step and $h^n_{i,j}$ is the hydraulic head at node point (i,j) after n time steps. As before, to obtain the sensitivity to the storativity in a zone containing several nodes, we must integrate Eq. (3.17) over that zone or sum the right side of Eq. (3.18) over the nodes in that zone.

$$\int_{\text{zone}_m}\left[\delta(x-x_k)\delta(y-y_\ell)\frac{\delta h}{\delta t}\right]^{n+1/2}_{\substack{x=x_i \\ y=y_j}} dA \simeq \sum_{\substack{k,\ell \\ \text{zone}_m}} \frac{(h^{n+1}_{i,j} - h^{n}_{i,j})}{\Delta t}\,\delta_{i,k}\delta_{j,\ell} \quad (3.19)$$

If numerical methods have been used to obtain the solution to Eq. (3.9), the flow equation, then the h's appearing in Eq. (3.15) or (3.19) are known and present no obstacle to a numerical solution of the equations for the sensitivity coefficients. The same numerical techniques used to solve the flow equation may be used to solve the sensitivity equations. In fact, the same computer code used for the flow equation can be used for the sensitivity equations by simply replacing the fluxes in Eq. (3.9) by the terms in Eq. (3.15) or (3.19). The system must be solved for each discrete value of x_o or zone. More discussion of the application of numerical methods to the solution of the sensitivity equations is given by McElwee (12). Ultimately, a numerical solution for the following sensitivity coefficients must be obtained.

$$U^n_{Ti,j;k,\ell} = \frac{\partial h^n_{i,j}}{\partial T_{k,\ell}} \tag{3.20}$$

$$U^n_{Si,j;k,\ell} = \frac{\partial h^n_{i,j}}{\partial S_{k,\ell}} \tag{3.21}$$

The superscript n is used to denote the nth time step while the subscripts i, j, k, and ℓ are the usual node indices. If zones are used, Eqs. (3.20) and (3.21) must be summed over all k and ℓ in that zone to obtain the total sensitivity to the parameter in that zone. Sometimes it is convenient to use only one subscript for the spatial variation and one for the transmissivity variation. In that case, the more compact forms for the sensitivity coefficients are $U^n_{Ti;k}$ and $U^n_{Si;k}$.

Along with the flow equation (3.9), initial conditions and boundary conditions must be given for h. An initial condition can be given in the form

$$h(x,y,0) - z = 0 \tag{3.22}$$

for a two-dimensional model. If Z is a constant, we have a flat initial surface. The boundary may be a rather arbitrary function of $\underline{x}$ denoted by

$$B(\underline{x}) = 0. \tag{3.23}$$

The boundary conditions must be specified on this curve. A specified head boundary is given by

$$[h(\underline{x},t)]_{B(\underline{x})} = H(\underline{x}). \tag{3.24}$$

If a specified flow of water is required on the boundary, then

$$\left[T(\underline{x}) \frac{\partial h(\underline{x},t)}{\partial n}\right]_{B(\underline{x})} = -Q''(\underline{x},t) \tag{3.25}$$

where $\partial/\partial n$ denotes the partial derivative in a direction normal to the boundary. If the constant is zero in Eq. (3.25), the result is a barrier boundary. In general, the boundary could contain both

types of boundary conditions given by Eqs.(3.24) and (3.25).

If the initial condition on h is a steady-state solution $U_S(\underline{x},0;\underline{x}_o)$, the initial condition on the sensitivity with respect to storage is zero. If z is a constant in (3.22), the initial condition on the sensitivity with respect to transmissivity, $U_T(\underline{x},0;\underline{x}_o)$, is also zero. If the initial surface is a steady-state solution, the initial condition $U_T(\underline{x},0;\underline{x}_o)$ is a solution to the steady-state form of Eq. (3.11) with the appropriate boundary conditions. The boundary conditions for U_T and U_S can be found by differentiating (3.24) and (3.25). For a specified head boundary

$$[U_T(\underline{x},t;\underline{x}_o)]_{B(\underline{x})} = 0 \tag{3.26}$$

$$[U_S(\underline{x},t;\underline{x}_o)]_{B(\underline{x})} = 0 \ . \tag{3.27}$$

A specified flow boundary condition results in

$$[T(\underline{x}) \frac{\partial U_T(\underline{x},t;\underline{x}_o)}{\partial n}]_{B(\underline{x})} = \delta(\underline{x}-\underline{x}_o)Q''(\underline{x},t) \tag{3.28}$$

$$[\frac{\partial U_S(\underline{x},t;\underline{x}_o)}{\partial n}]_{B(\underline{x})} = 0. \tag{3.29}$$

The sensitivity equations for the case of constant T and S can be obtained from Eqs. (3.11) and (3.17) by integrating over the whole model region.

$$U_T(\underline{x},t) = \int_R U_T(\underline{x},t;\underline{x}_o)\, dA \tag{3.30}$$

Performing this integration gives [McElwee and Yukler (11)]

$$T\frac{\partial}{\partial \underline{x}}[\frac{\partial U_T(\underline{x},t)}{\partial \underline{x}}] + \frac{\partial}{\partial \underline{x}}[\frac{\partial h(\underline{x},t)}{\partial \underline{x}}] = S\frac{\partial U_T(\underline{x},t)}{\partial t} \tag{3.31}$$

$$T\frac{\partial}{\partial \underline{x}}[\frac{\partial U_S(\underline{x},t)}{\partial \underline{x}}] = S\frac{\partial U_S(\underline{x},t)}{\partial t} + \frac{\partial h\ (\underline{x},t)}{\partial t} \ . \tag{3.32}$$

The boundary conditions for constant T and S are obtained by integrating Eqs. (3.26) to (3.29). For example, Eq. (3.28) becomes

$$\left[\frac{\partial U_T(\underline{x},t)}{\partial n}\right]_{B(\underline{x})} = \frac{Q''(\underline{x},t)}{T^2} . \tag{3.33}$$

4. EXAMPLES OF SENSITIVITY COEFFICIENTS

In the following sections, several examples of sensitivity coefficients will be shown. All the methods of determining sensitivity coefficients discussed in the previous sections will be illustrated.

4.1 The Theis Equation

The sensitivity coefficients for the Theis equation are given by Eqs. (3.2) and (3.3). The sensitivity coefficient for transmissivity, U_T, is shown in Figures 2 and 3 for a well pumping 32,000 ft^3/day with a transmissivity of 3,200 ft^2/day and a storage coefficient of .00095 at a time of .017 days. The radial dependence of U_T is shown in Figure 2. The system is obviously most sensitive to changes in the transmissivity near the well where drawdown is the largest. From Figure 2 the sensitivity coefficient U_T seems to diverge at the well. In fact, it may be shown from Eq. (3.3) that for $r^2S/4Tt \gg 1$,

$$U_T \simeq \frac{Q}{4\pi T^2}\left[1.577216 + \ln\left(\frac{r^2S}{4Tt}\right)\right]. \tag{4.1}$$

Expression (4.1) shows that U_T should diverge logarithmically at the well. The sensitivity function U_T changes sign in the region 300-

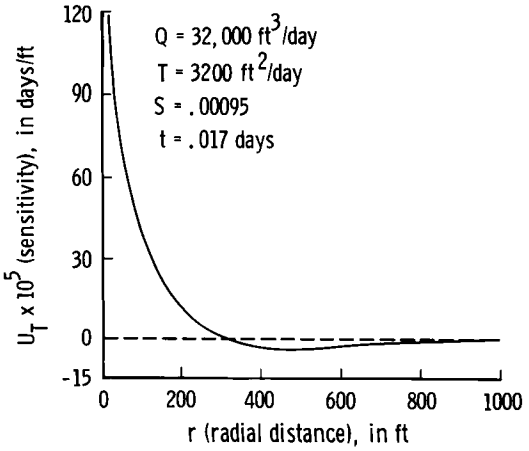

Fig. 2. Radial dependence of U_T for the Theis equation [McElwee and Yukler (11)].

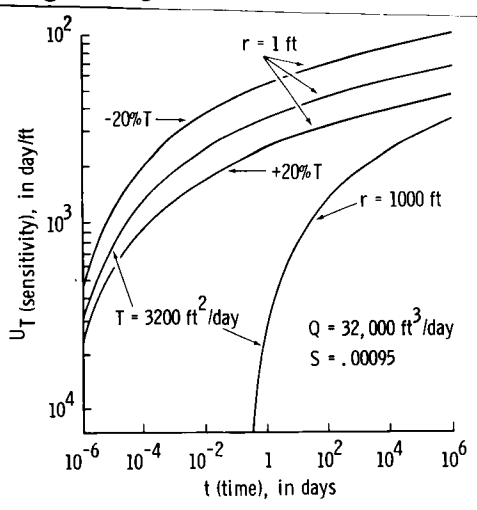

Fig. 3. Time dependence of U_T for the Theis equation [McElwee and Yukler (11)].

320 feet from the well, as it must in order for the cones of depression to have the same volume for differing transmissivities. The magnitude of the sensitivity coefficient U_T is relatively small in the region where U_T is negative.

Figure 3 shows a portion of the time dependence of U_T for two values of radius and two perturbed values of transmissivity. Notice that for large values of t, the dependence of U_T on t is fairly weak, though U_T is not constant. The curves labeled ±20% T show how U_T at a radius of 1 foot changes when the transmissivity is perturbed by ±20%. In this region a larger transmissivity results in decreased sensitivity, and a smaller transmissivity results in increased sensitivity. The curves labeled r = 1 foot and r = 1000 feet, for T = 3200 ft^2/day show the effect of changing r in the evaluation of U_T. These two curves have an identical shape but are displaced from one another along the t axis. The relation of these curves can be seen from Eq. (3.3). The critical ratio is r^2/t; as long as this ratio is the same, U_T will not change. Thus the curve for r = 1 foot at t = 10^{-6} days has the same value as the curve for r = 1000 feet at t = 1 day.

The sensitivity with respect to the storage coefficient, U_S, may be evaluated by using Eq. (3.2). The radial dependence of U_S is shown in Figure 4. U_S does not diverge at the well as does U_T. Eq. (3.2) and Figure 4 show that the radial dependence of U_S is Gaussian. U_S does not change sign because an increase or decrease in S results in a general raising or lowering, respectively, of the

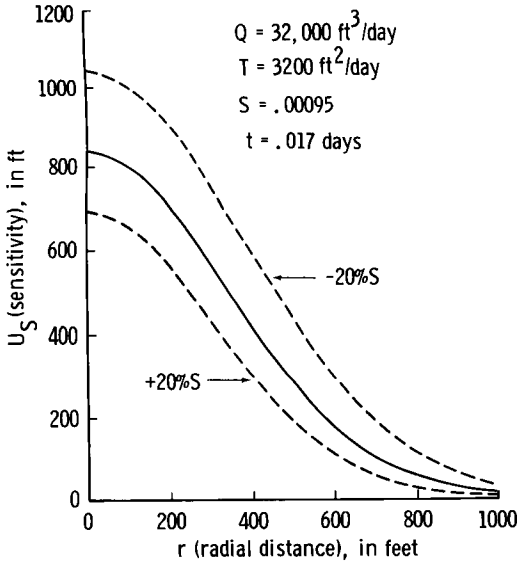

Fig. 4. Radial dependence of U_S for the Theis equation [McElwee and Yukler (11)].

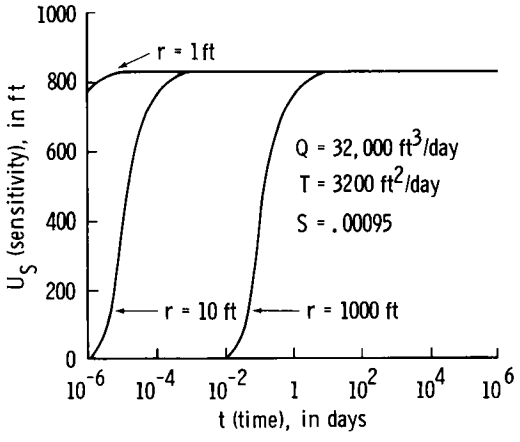

Fig. 5. Time dependence of U_S for the Theis equation [McElwee and Yukler (11)].

cone of depression. The dashed lines in Figure 4 show U_S when S is changed by ±20%. These curves indicate that the system is less sensitive for a larger S and more sensitive for a smaller S. This behavior can also be seen from Eq. (3.2).

The time dependence of U_S is illustrated in Figure 5 for three different r values. As time increases, U_S approaches a constant value. Even for r = 1000 feet, U_S is nearly constant after about 1 day. U_S is practically zero when the drawdown is very small and nearly constant after the drawdown attains 1-2 feet. The three curves shown in Figure 5 are identical except for displacement in time. From Eq. (3.2) it may be seen that U_S has the same value when r^2/t remains constant, provided Q, T, and S are unchanged. Thus the t = 1 day point on the curve for r = 1000 feet is identical to the t = 10^{-4} day point on the curve for r = 10 feet.

4.2 The Hantush Radial Leaky Aquifer

The sensitivity coefficients for the leaky aquifer are given by Eqs. (3.5), (3.6), and (3.8). U_T and U_S are evaluated by analytical expressions. U_L is obtained by a finite difference approximation. Many features of these sensitivity coefficients are similar to those found for the Theis equation. Therefore, description will be brief and new features will be pointed out. The sensitivity coefficients are shown in Figures 6 through 11 for Q = 196,000 ft^3/day, T = 24,300 ft^2/day, S = .002, and L = .0004 ft^{-1}.

The radial dependence of U_T is shown in Figure 6. The function diverges logarithmically near the well. U_T changes sign at some finite value of radius. This demonstrates the fact that when T is changed, the cone of depression deepens in some areas and shallows in others.

Figure 7 depicts a portion of the time dependence of U_T for variations in r and T. Note that U_T is inversely proportional to T. The curves represent a transmissivity of 24,300 ft^2/day and ±20% of that value at a radius of 100 feet and a T of 24,300 ft^2/day at a radius of 1,000 feet. Note that all curves flatten after three to four days. This describes the steady condition caused by deriving the discharge Q totally from leakage. This is a new effect that was not seen in the Theis case. In this case, U_T is constant after some time.

The radial dependence of U_S is shown in Figure 8. This coefficient does not diverge at the well, nor does it change sign. It is inversely proportional to S. The constancy of algebraic sign indicates that as S changes, a general raising or lowering of the cone of depression occurs.

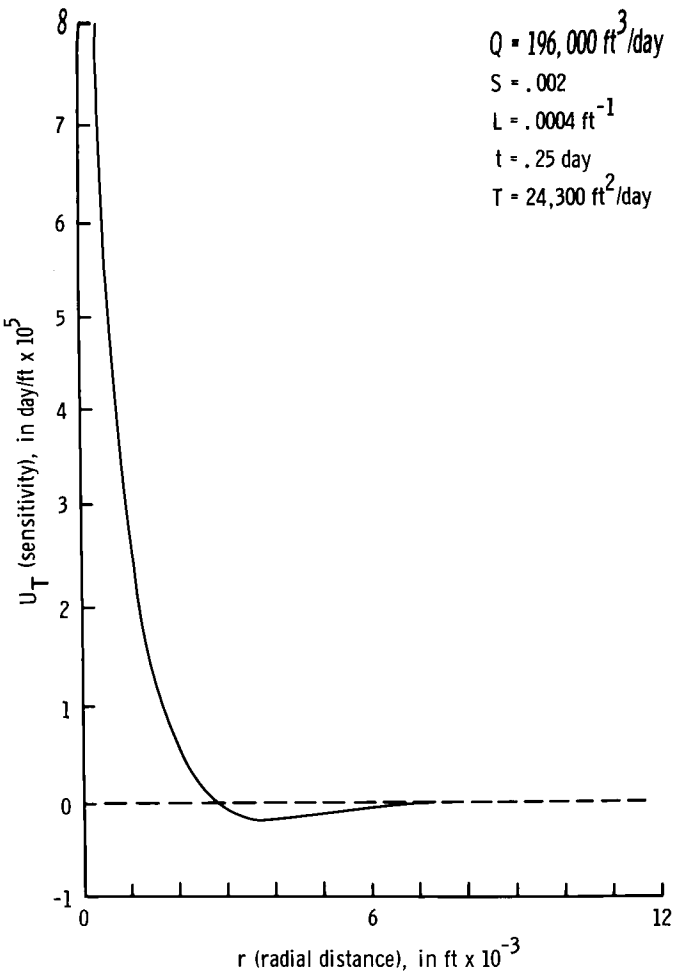

Fig. 6. Radial dependence of U_T for the leaky aquifer [Cobb, McElwee, and Butt (2)].

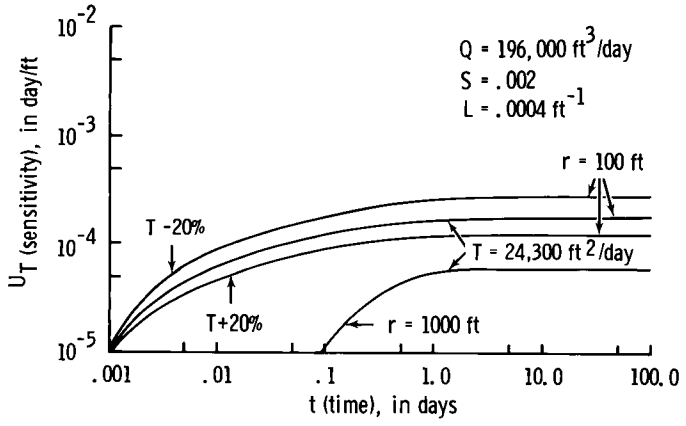

Fig. 7. Time dependence of U_T for the leaky aquifer [Cobb, McElwee, and Butt (2)].

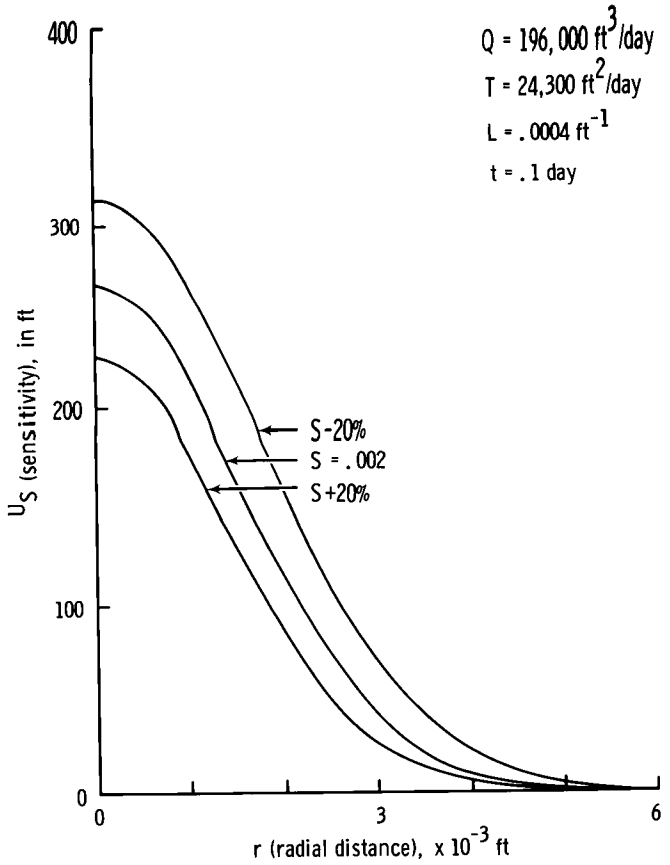

Fig. 8. Radial dependence of U_S for the leaky aquifer [Cobb, McElwee, and Butt (2)].

The time dependence of U_S is presented in Figure 9. Radial variation is indicated by the presence of three curves. Each curve reaches its maximum value for U_S at a time that increases with its radial value. At some finite value of time, each curve approaches zero in value, indicating that a steady state is achieved. Until steady state is attained, a dual source is supplying the pumpage, namely water released from storage and leakage. The curves roll over as leakage starts to dominate the source mechanism. U_S is zero outside the cone of depression and at any time after steady state is attained. Again, this is a new effect. U_S for the Theis model did not go to zero but approached a constant value for large times.

Figure 10 shows the radial dependence of U_L. The sensitivity coefficient U_L does not diverge at the well and approaches zero for large values of r. These are similar to the curves for U_S.

The time dependence of U_L is shown in Figure 11 for two values of r. All curves grow with time until a steady state is achieved where leakage is supplying the entire discharge Q. At that point, U_L is constant in time.

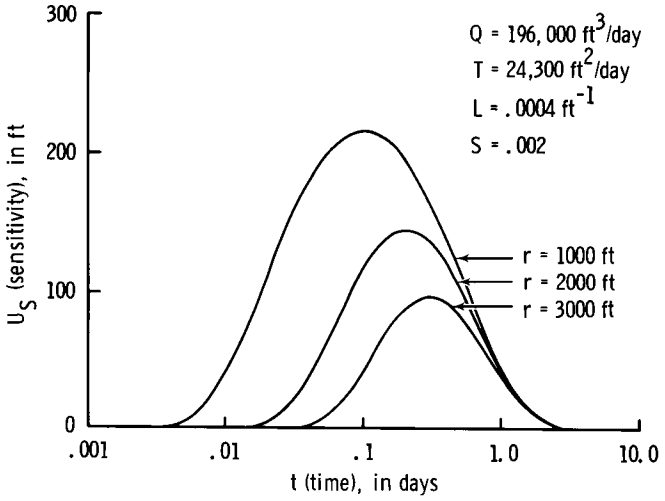

Fig. 9. Time dependence of U_S for the leaky aquifer [Cobb, McElwee, and Butt (2)].

In summary of the Theis and leaky aquifer sensitivity coefficients, a few observations can be made. The radial dependence of all the sensitivity coefficients (U_T, U_S, and U_L) shows that the greatest sensitivity is near the well and that the sensitivity approaches zero as the radial distance increases. The time dependence of all the sensitivity coefficients shows that initially the sensitivity grows with time. In the leaky case, U_S goes to zero as the steady state is approached while U_T and U_L approach constant values. In the Theis case, U_S approaches a constant value.

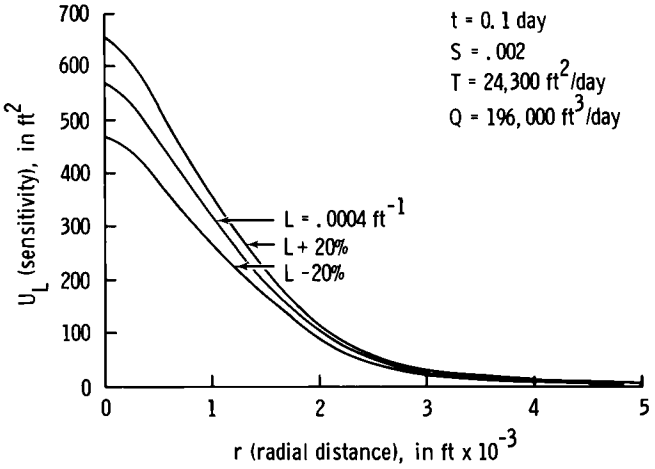

Fig. 10. Radial dependence of U_L for the leaky aquifer [Cobb, McElwee, and Butt (2)].

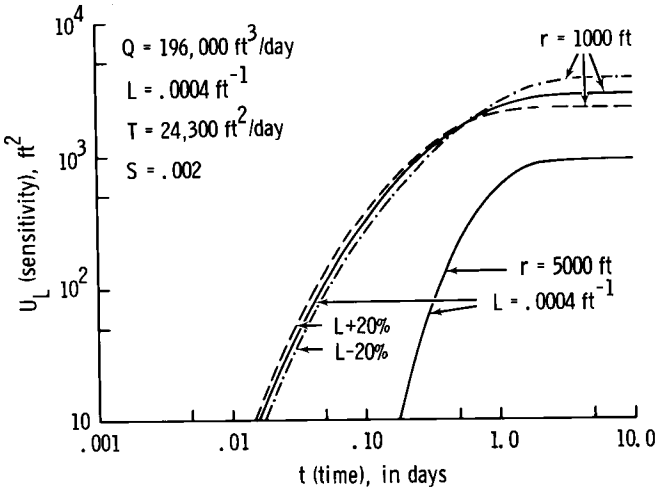

Fig. 11. Time dependence of U_L for the leaky aquifer [Cobb, McElwee, and Butt (2)].

4.3 One-Dimensional Model With Spatially Varying Transmissivity

Consider a steady state one-dimensional model with no interior fluxes. Eq. (3.9) becomes

$$\frac{\partial}{\partial x}\left[T(x)\,\frac{\partial h}{\partial x}\right] = 0. \tag{4.2}$$

The first integration of Eq. (4.2) gives

$$T(x)\,\frac{\partial h}{\partial x} = C = \text{constant}. \tag{4.3}$$

For boundary conditions, assume

$$h = H \quad \text{at } x = R \tag{4.4}$$

and

$$\frac{\partial h}{\partial x} = -\frac{Q/\ell}{T(0)} \quad \text{at } x = 0. \tag{4.5}$$

Q/ℓ is the boundary flux per unit length of boundary. Integration of Eq. (4.3) yields the final solution for the hydraulic head

$$h(x) = \frac{QR}{\ell} \int_{x/R}^{1} \frac{dx'}{T(Rx')} + H. \tag{4.6}$$

The normalized variable $x' = x/R$ has been introduced. Eq. (4.6) allows for an arbitrary distribution of the transmissivity.

Consider the case of constant transmissivity in Eq. (4.6). The solution is

$$h(x) = \frac{Q}{\ell T} (R-x) + H. \tag{4.7}$$

Using the definition of U_T from the Eq. (2.7) yields

$$U_T(x) = \frac{\partial h(x)}{\partial T} = \frac{Q}{\ell T^2} (x-R) = - \frac{s}{T}, \tag{4.8}$$

where s is the drawdown with reference to the constant head boundary.

$$s = h(x) - H = \frac{Q}{\ell T} (R-x) \tag{4.9}$$

This form [Eq. (4.8)] of the sensitivity coefficient is rather common [see Eqs. (3.3) and (3.6)] and merely says that the model is more sensitive to transmissivity in areas having larger drawdown. Notice that, as the constant head boundary is approached, the sensitivity coefficient (U_T) goes to zero. The sensitivity with respect to storativity, U_S, is zero since only the steady state is being considered.

The sensitivity coefficients for an arbitrary transmissivity distribution can be found by considering the head solution, Eq. (4.6), and the definition of the sensitivity coefficient, Eq. (2.12). The new head caused by changing the transmissivity at one point (x_o) is

$$h^*(x) = \frac{QR}{\ell} \int_{x/R}^{1} \frac{dx'}{T(Rx') + \delta(Rx'-x_o)\Delta T(x_o)}. \tag{4.10}$$

The sensitivity coefficient developed from (2.12) is as follows

$$U_T(x;x_o) = \begin{cases} -\frac{QR}{\ell}\frac{1}{T^2(x_o)} & \text{if } x \leq x_o \leq R \\ 0 & \text{if } x_o < x \end{cases} . \qquad (4.11)$$

This sensitivity coefficient is inversely proportional to the square of the transmissivity. Thus, areas of low transmissivity have a larger effect on model results than areas of high transmissivity. Also, notice that the transmissivity of x_o values less than the observation point, x, do not affect model results at the observation point. The sensitivity coefficient resulting from changing the transmissivity, a constant amount ΔT over the whole model area [Eq. (2.16)] is obtained by integrating Eq. (4.11).

$$U_T(x) = \int_0^1 U_T(x;Rx'_o)\, dx'_o = -\frac{QR}{\ell}\int_{x/R}^1 \frac{dx'_o}{T^2(Rx'_o)} \qquad (4.12)$$

The normalized integration variable $x'_o = x_o/R$ has been introduced. If the transmissivity is constant, Eq. (4.12) becomes identical with Eq. (4.8).

Typically, numerical methods are used to solve the model equations when the transmissivity is allowed to vary in an arbitrary manner. Assume a constant node spacing (Δx) grid system has been set up such that $N\Delta x = R$, where N+1 is the total number of nodes (x = 0 is the first node). The head at point x_i ($x_i = i\Delta x$) is obtained from Eq. (4.6) by the following replacement.

$$R \int_{x_i/R}^1 dx' \rightarrow \Delta x \sum_{k=i}^N \qquad (4.13)$$

Assuming that a constant transmissivity exists between points k and k+1 ($T_{k+1/2}$), Eq. (4.6) becomes

$$h_i = \frac{Q\Delta x}{\ell}\sum_{k=i}^N \frac{1}{T_{k+1/2}} + H. \qquad (4.14)$$

The sensitivity coefficient is obtained by differentiating Eq. (4.14).

$$U_{Ti;k} = \frac{\partial h_i}{\partial T_{k+1/2}} = \begin{cases} -\frac{Q\Delta x}{\ell}\frac{1}{T^2_{k+1/2}} & \text{if } k \geq i \\ 0 & \text{otherwise} \end{cases} \qquad (4.15)$$

this result could have been obtained from Eq. (4.11) simply by integrating the effect of a constant transmissivity over one node spacing. The sensitivity coefficient $U_{Ti;k}$ represents the change in hydraulic head at node point i due to a change in the transmissivity at k+ 1/2.

Consider a specific example of Eqs. (4.14) and (4.15). Assume $Q\Delta x/\ell = 10^3$, N = 9, H = 1, and $T_{k+\ 1/2} = (k+1) \times 10^3$. Figure 12 is a plot of the head and Figure 13 is a plot of the absolute value of various sensitivity coefficients. All sensitivity coefficients are zero at node 10 where the head is specified. Since the magnitude of the sensitivity coefficients is inversely proportional to the transmissivity squared, the coefficients decrease dramatically as the transmissivity increases from node 0 to node 9.

4.4 A Simple Two-Dimensional Model With Spatially Varying Transmissivity

For a first look at two-dimensional sensitivity coefficients we use a simple two-dimensional flow model shown in Figure 14. This model has two zones for transmissivity and recharge. There are 25 node points with a node spacing of 500 in the y direction and 1000 in the x direction. Transmissivities of 1000 for zone one and 2000 for zone two are chosen. The recharge is .00625 and .003125 for zones one and two, respectively. No units have been given since any consistent set may be used.

The boundary conditions remain to be specified. Assume that the flux is specified on the x = 0 boundary and that the head is specified on the other three boundaries. Let the flux per unit

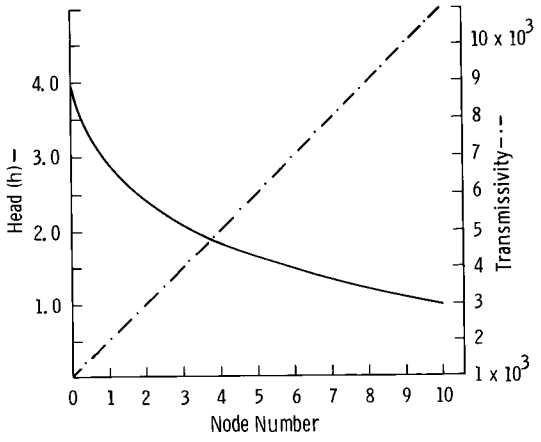

Fig. 12. Head and transmissivity for a simple one-dimensional model.

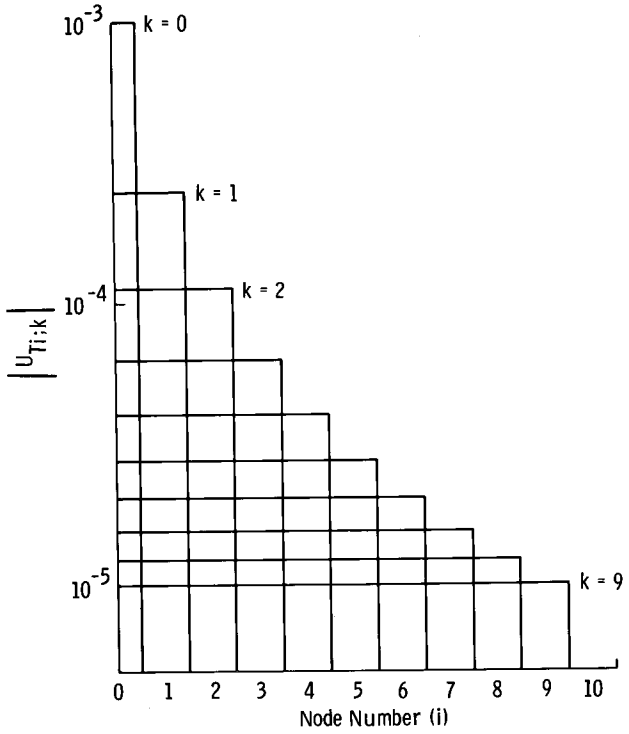

Fig. 13. Sensitivity coefficients for a simple one-dimensional model.

length (Q/ℓ) of the boundary at x = 0 be -50 units (out of the model area). For simplicity, assume the flow is parallel to the x axis and that the head at nodes 1 and 21 is 100. This allows the appropriate head to be specified for all the other boundary nodes. The values are shown in Table 1.

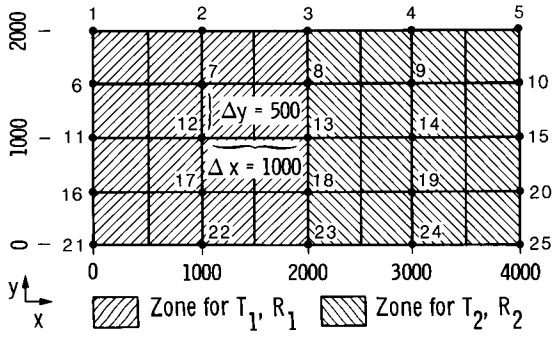

Fig. 14. A simple two-dimensional model.

Table 1. Head values for boundary nodes.

Head	Node Number
100	1, 21
146.9	2, 22
187.5	3, 23
205.5	4, 24
221.9	5, 10, 15, 20, 15

The sensitivity coefficients for the transmissivities in the two zones are shown in Figures 15 and 16. Notice that the coefficients are zero on the head-specified boundaries. Of course, this is required by Eq. (3.26). Also notice that the sensitivity coefficients have their largest magnitudes either in the middle of the flow-specified boundary or in the middle of the model.

5. EFFECT OF BOUNDARY CONDITIONS ON SENSITIVITY COEFFICIENTS

Boundary conditions have an effect on the shape and magnitude of the sensitivity coefficients. This is shown explicitly by Eqs. (3.26) - (3.29). The examples in sections 4.3 and 4.4 were affected by the boundary conditions chosen; however, in those sections, alternate boundary conditions were not shown. The purpose of this section is to compare sensitivity coefficients for various choices of boundary conditions. The examples chosen will be closely related to the examples of previous sections.

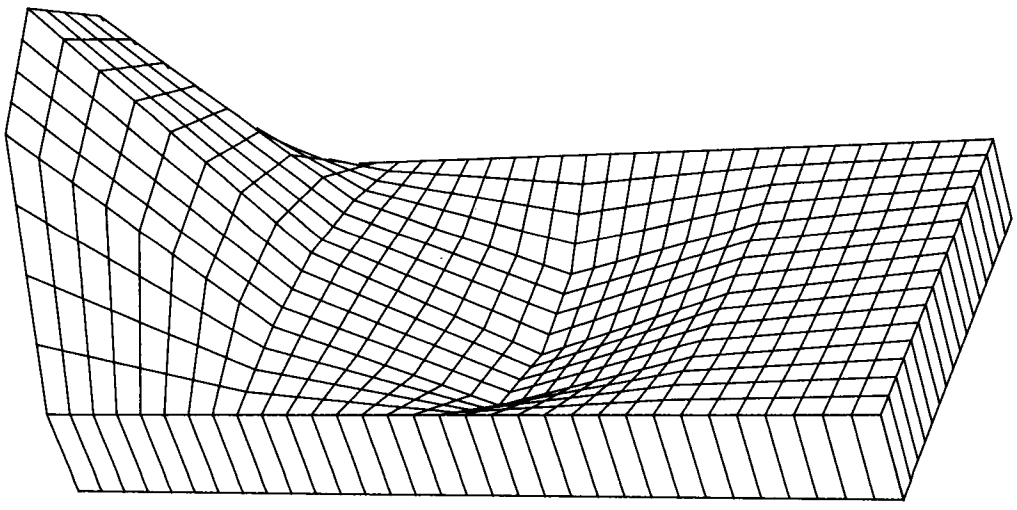

Fig. 15. Sensitivity coefficient for transmissivity in zone one.

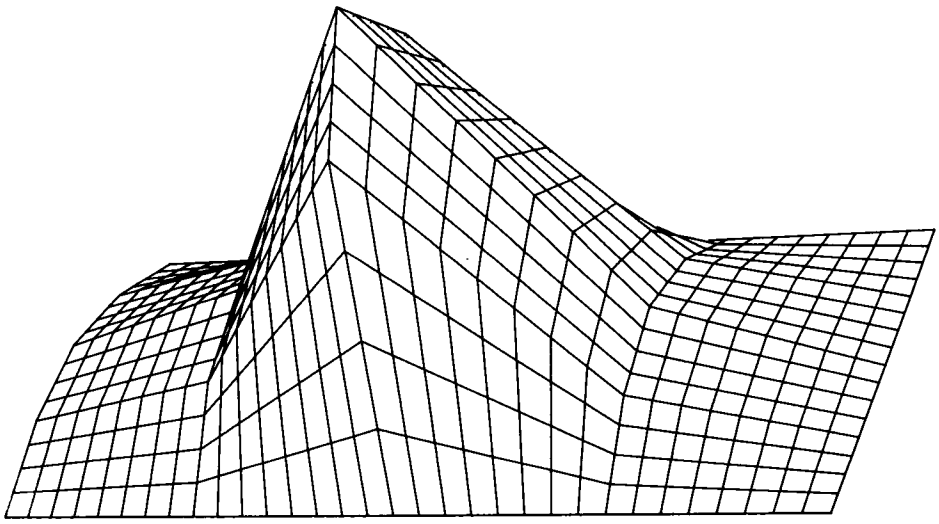

Fig. 16. Sensitivity coefficient for transmissivity in zone two.

5.1 Finite Radial Confined Aquifer

The values of the parameters Q, T, and S for the finite radial numerical model were chosen to be the same as those used in the Theis equation of section 4.1. However, two additional parameters are needed: the radius of the well and the radius of the outer boundary. The radius of the well was taken as 1 foot; and an outer boundary of 10,000 feet was used. The numerical results for U_T, obtained by choosing a constant head boundary or a barrier boundary at 10,000 feet, are shown in Figure 17 along with U_T calculated from the Theis equation. For times less than about 10 days, no difference exists in the three curves for r = 1 foot and for r = 1000 feet.

The constant head boundary at 10,000 feet produces a U_T as shown by the dot-dash curves in Figure 17. The Theis infinite model results are shown as a solid curve. For times greater than about 20 days, the water level is static owing to the constant head boundary, and U_T obtains a constant value in time. The radial dependence of U_T at steady state is a straight line when it is plotted versus log r and goes to zero at the outer boundary where the drawdown is zero.

Note that U_T at steady state is positive for all r. This is to be contrasted with the U_T shown in Figure 2 for the Theis equation. The fact that U_T is positive is a direct consequence of the fact that all the water being pumped is supplied by the constant head boundary; no water is being supplied from storage. Increasing

or decreasing T results in a general raising or lowering, respectively, of the hydraulic head at steady state.

The numerical solution for U_T with a barrier boundary condition at 10,000 feet is shown by the dashed curves in Figure 17. After about 10 days, the cone of depression has reached the barrier boundary and U_T becomes constant in time.

In Figure 18 the radial dependence of U_T (for a barrier boundary) is shown for time considerably greater than 10 days, i.e., for time such that U_T is constant in time. Notice that U_T is negative for r greater than about 5500 feet. This is to be contrasted with a positive U_T for a constant head boundary. Because no water can flow into the system with a barrier boundary, all water pumped must come from storage. Thus, for two systems with differing T and the same Q, the cones of depression must contain the same volume at any given instant. The low T system will have a larger drawdown near the well and a smaller drawdown far from the well, because the lower T impedes the flow to the well. This explains why U_T has both negative and positive areas. A change in T will produce greater drawdown in one area and less drawdown in another area.

Figure 19 compares U_S calculated from the Theis equation (solid curve) with U_S calculated numerically for a constant head boundary

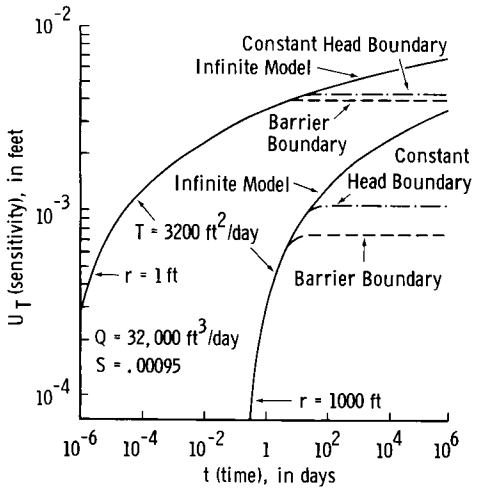

Fig. 17. Effect of the boundary at 10,000 ft on U_T [McElwee and Yukler (11)].

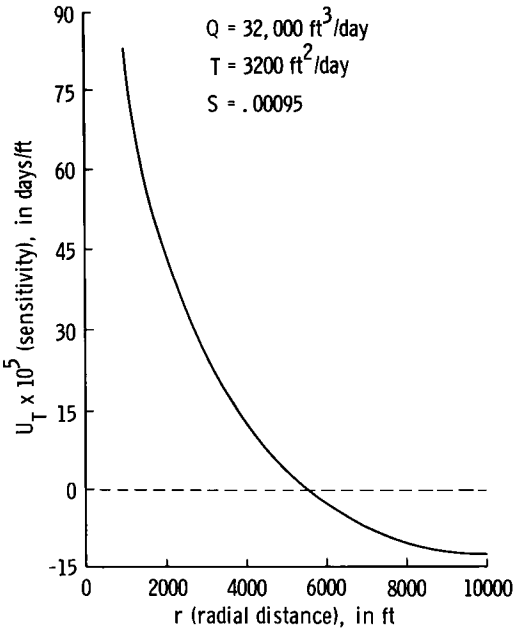

Fig. 18. Radial dependence of U_T at large time for a barrier boundary at 10,000 ft [McElwee and Yukler (11)].

(dot-dash curve) or a barrier boundary (dashed curve) at 10,000 feet. From the earlier discussion, remember that the water level does not change much after 20 days for the constant head boundary condition (approximately steady state). From Figure 19 we see that U_S for the constant head boundary is approximately zero after about 100 days. This behavior of U_S is to be expected, since the solution at steady state is independent of S because no water is coming from storage then.

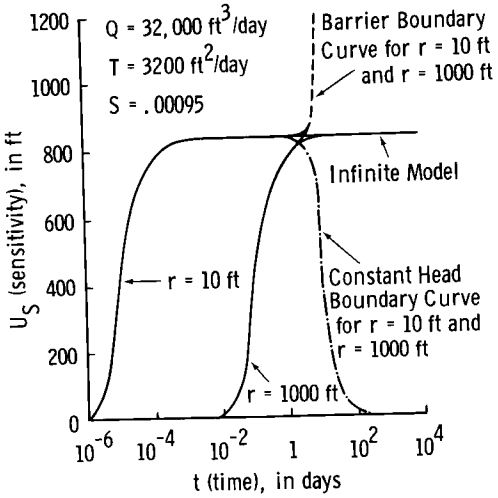

Fig. 19. Effect of the boundary at 10,000 ft on the time dependence of U_S [McElwee and Yukler (11)].

All values of U_S plotted in Figure 19 are positive, indicating that an increase or decrease of S results in a general raising or lowering, respectively, of the hydraulic head. U_S for the barrier boundary condition increases dramatically after a few days time, as is shown in Figure 19. U_s increases linearly with time after about 10 days. Numerical results indicate that U_S is the same for all values of r after about 10 days. The linear increase of U_S with time is due to the fact that the hydraulic head decreases uniformly with time after about 10 days. In short, the system becomes increasingly sensitive to S as the barrier boundary exerts a greater influence on the drawdown.

To summarize, a number of effects have been observed due to boundary conditions. U_T becomes constant after some time and U_S either goes to zero or increases linearly with time as the influence of the boundary is felt. A great deal of similarity exists between the leaky aquifer case of section 4.2 and the constant head boundary results presented here. U_T becomes constant and U_S goes to zero in both cases. On the other hand, U_S increases linearly with time for the barrier boundary at long times. This points out that each system has a characteristic behavior, and sensitivity analysis can help understand that behavior.

5.2 Alternate Boundary Conditions For The One-Dimensional Aquifer

In section 4.3, an analytical expression was derived for the sensitivity with respect to transmissivity for a steady-state one-dimensional model with spatially varying transmissivity and certain boundary conditions. Those sensitivity coefficients were shown in

Figure 13. In this section, the same system will be used except for differing boundary conditions.

Consider a steady-state one-dimensional model with the head specified at both boundaries.

$$h = H_1 \text{ at } x = 0 \tag{5.1}$$

$$h = H_2 \text{ at } x = R \tag{5.2}$$

Eqs. (4.2) and (4.3) are still valid for this model. Integrating Eq. (4.3) yields

$$h(x) = C \int_{x/R}^{1} \frac{dx'}{T(Rx')} + H_2 , \tag{5.3}$$

where C is a constant to be determined from the boundary condition at x = 0. Putting x = 0 in Eq. (5.3) results in the following expression for C.

$$C = (H_1-H_2)/ \int_{0}^{1} \frac{dx'}{T(Rx')} \tag{5.4}$$

If T is constant, Eqs. (5.3) and (5.4) yield

$$h(x) = \left(\frac{H_2-H_1}{R}\right) x + H_1 . \tag{5.5}$$

Since Eq. (5.5) does not depend on the transmissivity,

$$U_T(x) = \frac{\partial h(x)}{\partial T} = 0. \tag{5.6}$$

When the transmissivity is not constant, the sensitivity coefficients can be obtained by applying the definition, Eq. (2.12),

$$U_T(x;x_o) = [h(x)-H_2 + (H_2-H_1)\theta(x-x_o)]/[T^2(x_o) \int_{0}^{1} \frac{dx'}{T(Rx')}]. \tag{5.7}$$

$\Theta(x_o-x)$ is the Heaviside unit step function.

$$\Theta(x_o-x) = \begin{cases} 1 & \text{if } x_o \geq x \\ 0 & \text{if } x_o < x \end{cases} \tag{5.8}$$

h(x) is given by Eqs. (5.3) and (5.4). Eq. (5.7) shows that $U_T(x;x_o)$ has both negative and positive areas. If we assume that $H_1 \geq h(x) \geq H_2$, then $U_T(x;x_o)$ negative for $x_o \geq x$ and positive for $x_o < x$. If T is constant $U_T(x)$ is zero, as was already known from Eq. (5.6). Thus, the model becomes less sensitive to the value of T as a constant value of T is approached.

The numerical solution for the above model with constant node spacing (Δx) may be obtained as before by replacing the integrals in Eqs. (5.3) and (5.4) with the appropriate summations.

$$h_i = \frac{(H_1 - H_2)}{\sum_{k=0}^{N} \frac{1}{T_{k+1/2}}} \sum_{k=i}^{N} \frac{1}{T_{k+1/2}} + H_2 \tag{5.9}$$

The sensitivity coefficient $U_{Ti;k}$ can be obtained from Eq. (5.9) by differentiation.

$$U_{Ti;k} = [h_i - H_2 + (H_2 - H_1)\Theta(k-i)] / [T_{k+1/2}^2 \sum_{\ell=0}^{N} \frac{1}{T_{k+1/2}}] \tag{5.10}$$

This equation is the discrete equivalent of Eq. (5.7). $U_{Ti;k}$ represents the change in hydraulic head at node point i due to a change in transmissivity at k+1/2. Eq. (5.10) can be written in slightly different form.

$$U_{Ti;k} = 1/[T_{k+1/2}^2 \sum_{\ell=0}^{N} \frac{1}{T_{\ell+1/2}}] \begin{cases} (h_i - H_2) & \text{if } k < i \\ (h_i - H_1) & \text{if } k \geq i \end{cases} \tag{5.11}$$

This form shows that the sensitivity coefficients can be determined from just two functions, $T_{1/2}^2 U_{Ti;0}$ and $T_{N+1/2}^2 U_{Ti;N}$. All other sensitivity coefficients can be generated from these two. When k = i, $T_{k+1/2}^2 U_{Ti;k}$ switches from one curve to the other.

As an example of Eq. (5.11), consider the simple model of section 4.3, i.e., N = 9, and $T_{k+1/2} = (k+1) \times 10^3$. This time the head will be specified at both ends. From Figure 12 we can see that $H_1 = 3.93$ and $H_2 = 1.0$. Figure 20 shows a plot of $T^2_{1/2}\, U_{Ti;0}$ and $T^2_{9+1/2}\, U_{Ti;9}$; in addition, $T^2_{4+1/2}\, U_{Ti;4}$ is shown to illustrate the crossover between the two curves. Notice that the sensitivity coefficients are zero at both boundaries since head is specified there. $U_{Ti;0}$ is everywhere positive while $U_{Ti;9}$ is everywhere negative. All the other sensitivity coefficients have some negative and some positive areas. These sensitivity coefficients are very different from those shown in Figure 13; yet the only difference in the models is that the head is specified at the left boundary in this case.

5.3 Alternate Boundary Conditions For The Simple Two-Dimensional Model

For the model defined in section 4.4 and Figure 14, it is possible to specify different boundary conditions and observe the effect on the sensitivity coefficients. First, let the boundaries at y = 0 and y = 2000 be barrier boundaries instead of head-specified boundaries. The resulting sensitivity coefficients are shown in Figures 21 and 22. Notice that the sensitivity coefficients no longer show a variation in the y direction. If, in addition to the barrier boundaries at y = 0 and y = 2000, the flow-specified boundary at x = 0 is changed to a head-specified boundary, the resulting sensitivity coefficients are shown in Figures 23 and

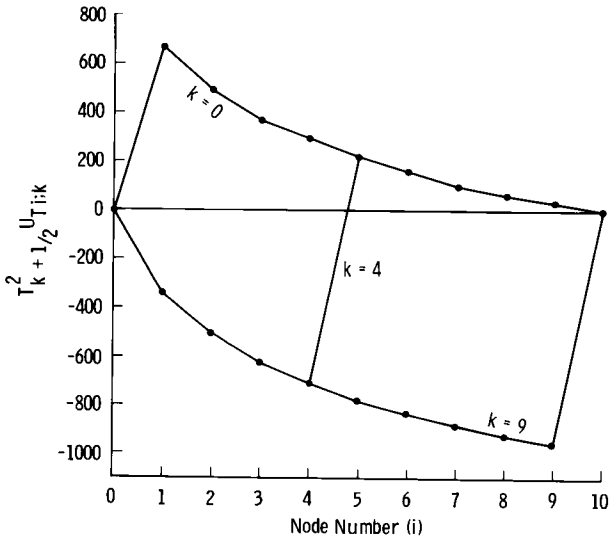

Fig. 20. Sensitivity coefficients for the one-dimensional model with head specified on both ends.

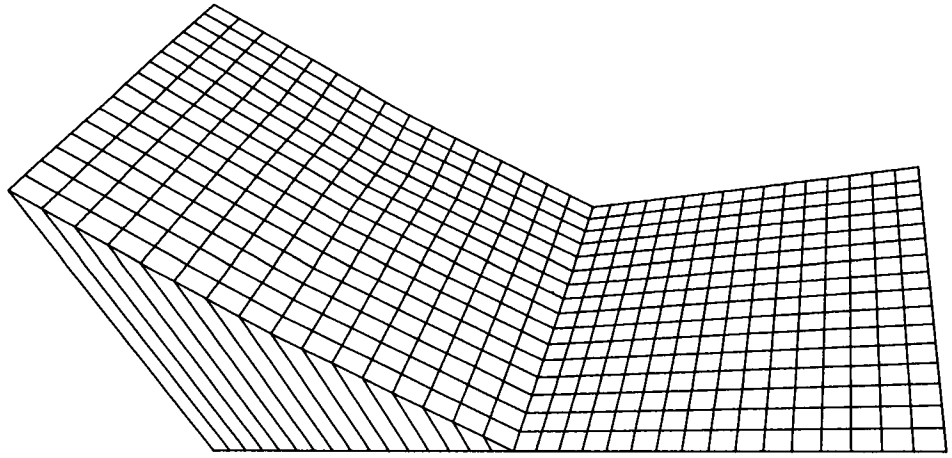

Fig. 21. Sensitivity coefficient for transmissivity in zone one, barrier boundaries at y = 0 and y = 2000.

24. It is very clear from these examples that the boundary conditions exert a large influence on the sensitivity coefficients.

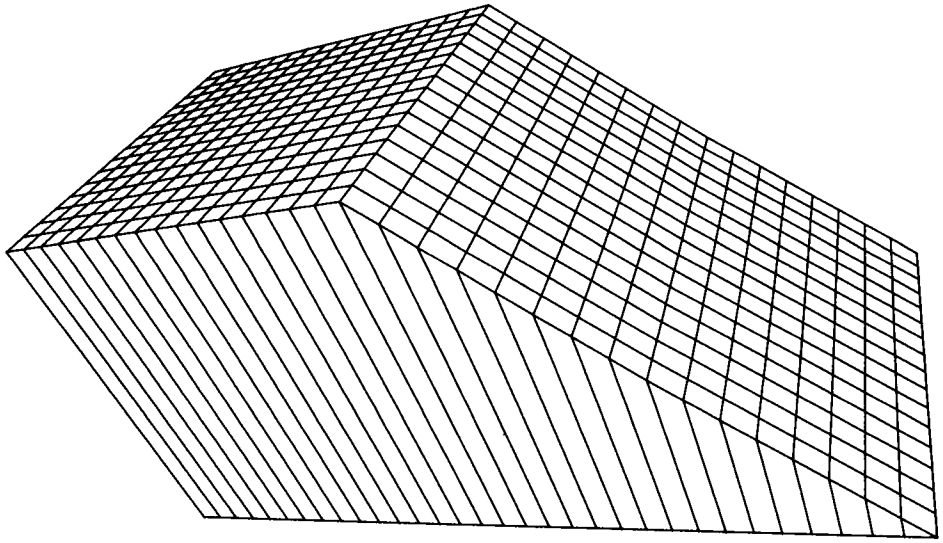

Fig. 22. Sensitivity coefficient for transmissivity in zone two, barrier boundaries at y = 0 and y = 2000.

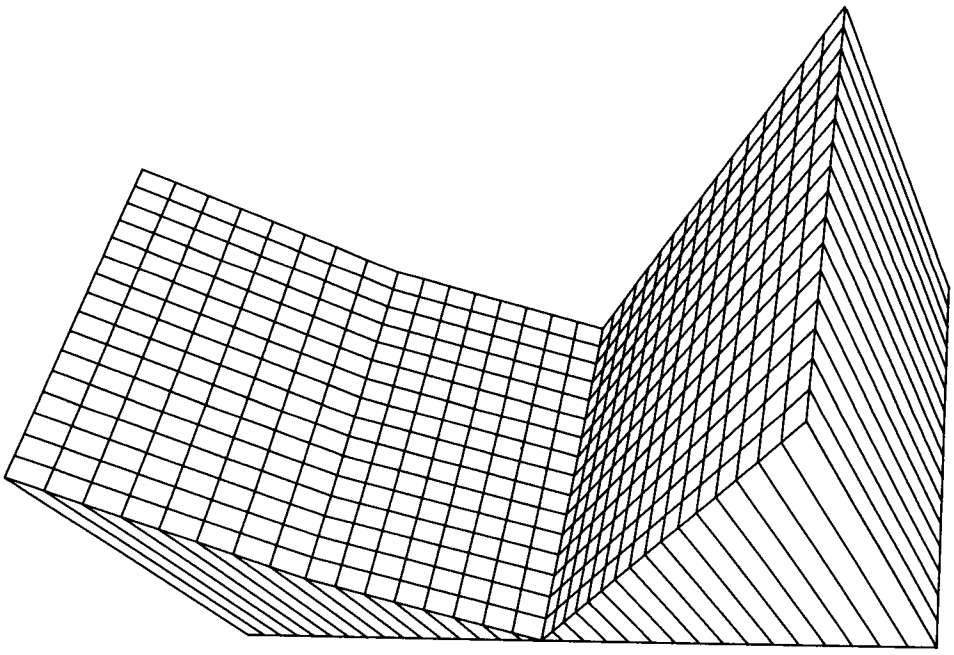

Fig. 23. Sensitivity coefficient for transmissivity in zone one for barrier boundaries at y = 0 and y = 2000 and head specified at x = 0 and x = 4000.

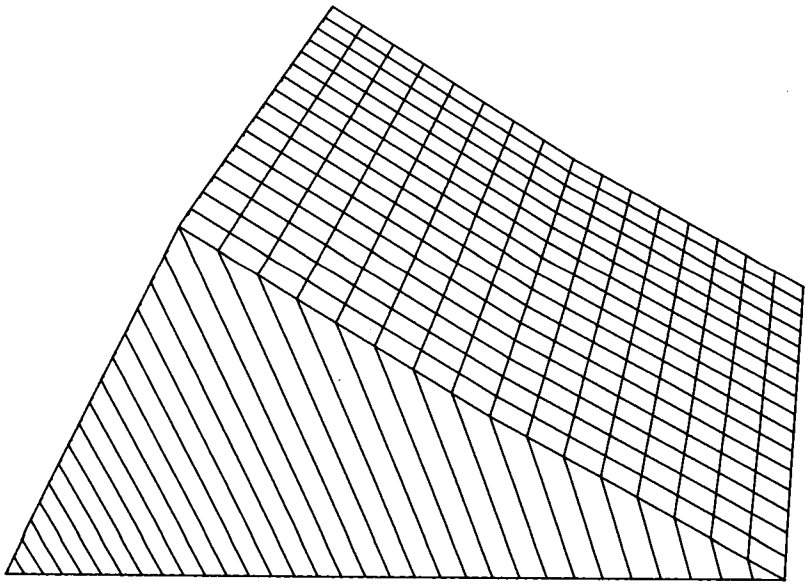

Fig. 24. Sensitivity coefficient for transmissivity in zone two for barrier boundaries at y = 0 and y = 2000 and head specified at x = 0 and x = 4000.

6. THE ROLE OF SENSITIVITY COEFFICIENTS IN PARAMETER ESTIMATION

The so-called "indirect" inverse procedures attempt to calculate the "best" transmissivity and storativity by minimizing some error functional [Cooley (3), Cooley (4), Neuman and Yakowitz (15), and Neuman (16)]. In this case, the aquifer parameters which are obtained by minimization do not exactly satisfy the direct equations. Rather, the best average solution is obtained over the historical period of record. Suppose that initial estimates for T and S can be made, and that h_i^n is the head calculated from the model at node point i and time step n. If all the aquifer parameters are changed by some amount (ΔT_k or ΔS_k, k is the zone index), the new head h_i^{*n} is given by

$$h_i^{*n} = h_i^n + \sum_k^{M_1} U_{Ti;k}^n \, \Delta T_k + \sum_k^{M_2} U_{Si;k}^n \, \Delta S_k \qquad (6.1)$$

where M_1 is the number of T zones and M_2 is the number of S zones. $U_{Ti;k}^n$ represents the change in head at node i for time step n due to a change in the transmissivity in zone k. A similar definition applies for $U_{Si;k}^n$. These are the sensitivity coefficients that have been discussed at length in earlier sections.

6.1 Ordinary Least Squares

If he_i^n is the experimentally measured head at node point i for time step n, it would be desirable to choose ΔT_k and ΔS_k in such a way as to minimize the difference between h* and he. The error functional chosen to be minimized is the sum of the squared errors over all node points and time steps.

$$E(\Delta T_k, \Delta S_k) = \sum_n \sum_i \left[he_i^n - h_i^{*n} \right]^2 \qquad (6.2)$$

This error functional assumes that measurement accuracy and any other source of error is the same for all points and times. (If this is not true, a weighting function could be used. If a weighting function other than one is used, we have generalized least squares, which will be discussed briefly in the next section.)

A necessary condition for minimization of $E(\Delta T_k, \Delta S_k)$ is that the partial derivatives with respect to ΔT_k or ΔS_k be zero. We can drop the subscript T and S on $U_{Ti;k}^n$ and $U_{Si;k}^n$ without ambiguity by letting k go from one to $M_1 + M_2 = p$. In general, the number and locations of the zones for T and S will be different.

$$U^n_{i;k} = \begin{cases} U^n_{Ti;k} & k \leq M_1 \\ U^n_{Si;k} & M_1 < k \geq M_2 \end{cases} \tag{6.3}$$

$\sum_n U^n_{i;k}$ can now be considered as one element of the matrix $\underset{\sim}{U}$. Note that, in general, $\underset{\sim}{U}$ is not a square matrix. Similarly define a parameter vector, $\underline{P}$. Note, + indicates the transpose of a vector or matrix.)

$$\underline{P}^+ = [T_1, T_2, \cdots T_{M_1}, S_1, S_2, \cdots S_{M_2}] \tag{6.4}$$

The minimization condition can now be written as [Beck and Arnold (1)]

$$(\underset{\sim}{U}^+\underset{\sim}{U})\underline{\Delta P} = \underline{R} \tag{6.5}$$

or

$$\underline{\Delta P} = (\underset{\sim}{U}^+\underset{\sim}{U})^{-1}\,\underline{R} \tag{6.6}$$

where $\underline{\Delta P}$ is a vector of parameter changes required to minimize the functional. One element of the vector $\underline{R}$ (R_k) is given by

$$R_k = \sum_n \sum_i U^n_{i;k}\,(he^n_i - h^n_i). \tag{6.7}$$

Any standard matrix routine may now be used to solve Eq. (6.5) for the parameter changes which will minimize the error functional. Since it is a nonlinear problem ($\underset{\sim}{U}$ depends on $\underline{P}$), iteration until convergence occurs is necessary; i.e., until $\underline{\Delta P}$ approaches zero.

In order to perform a more detailed statistical analysis on the parameter reliability, it is necessary to find the parameter covariance matrix. For ordinary least squares and certain statistical assumptions (additive, zero mean, uncorrelated and constant variance errors), the parameter covariance is given by [Beck and Arnold (1)]

$$\underset{\sim}{P} = \text{cov}\,(\underline{P}) \approx (\underset{\sim}{U}^+\underset{\sim}{U})^{-1}\sigma^2 \tag{6.8}$$

where σ^2 is the head error variance. The estimated standard error of the parameters is given by the square root of the diagonal

elements of the matrix $\underset{\sim}{P}$ in Eq. (6.8).

$$\text{Estimated Standard Error of } P_k = P_{kk}^{1/2} \tag{6.9}$$

If σ^2, the head error variance, is unknown, it can be approximated by

$$\sigma^2 \simeq s^2 = \sum_n \sum_i [he_i^n - h_i^{*n}]^2/(m-p) \tag{6.10}$$

where m is the total number of observations in space and time and p is the number of parameters to be estimated.

The approximate parameter correlation matrix, which shows the degree of dependence among parameters, can be found from Eq. (6.8). An element of the matrix has the form [Beck and Arnold (1)]

$$r_{ik} = P_{ik} (P_{ii} P_{kk})^{-1/2}. \tag{6.11}$$

The diagonal elements are all unity. The off-diagonal elements are between -1 and 1. As the magnitude of an off-diagonal element approaches one, it indicates a high correlation between parameters. When this occurs, the two parameters are nearly dependent and it may not be possible to estimate both.

6.2 Other Methods

One might possibly want to weight some measurements more than others. Also some prior information may exist on the aquifer parameters. In these cases, the function to be minimized would not be given by Eq. (6.2) but by a more general function such as [Beck and Arnold (1)]

$$E(\Delta T_k, \Delta S_k) = [\underline{he}-\underline{h}^*]^+ \underset{\sim}{W} [\underline{he}-\underline{h}^*] + [\underline{P}-\underline{P}_o]^+ \underset{\sim}{V} [\underline{P}-\underline{P}_o] \tag{6.12}$$

where

$$[\underline{he}-\underline{h}^*] = [(he_1^1 - h_1^1), \cdots (he_i^n - h_i^{*n}) \cdots]. \tag{6.13}$$

$\underset{\sim}{W}$ is the weight matrix for head measurements, $\underline{P}_o$ is the vector of prior estimates for the aquifer parameters, and $\underset{\sim}{V}$ is the weight matrix for the prior estimates. $\underset{\sim}{W}$ is a symmetric square matrix whose dimensions are equal to the total number of head measurements. $\underset{\sim}{V}$ is a symmetric square matrix with dimensions equal to the number of prior estimates. By the proper choice of $\underset{\sim}{W}$ and $\underset{\sim}{V}$ one can perform weighted least squares (WLS) estimation, maximum likelihood (ML)

estimation, or maximum a posteriori (MAP) estimation.

In this more general case, the extension of Eq. (6.6) becomes

$$\Delta\underline{P} = [\underset{\sim}{U}^{+}\underset{\sim}{W}\,\underset{\sim}{U} + \underset{\sim}{V}]^{-1}[\underset{\sim}{U}^{+}\underset{\sim}{W}(\underline{he} - \underline{h}^{*}) + \underset{\sim}{V}(\underline{P} - \underline{P}_{o})]. \tag{6.14}$$

The parameter covariance matrix Eq. (6.8) must also be extended.

$$\underset{\sim}{P} = \mathrm{cov}(\underline{P}) \simeq [\underset{\sim}{U}^{+}\underset{\sim}{W}\,\underset{\sim}{U} + \underset{\sim}{V}]^{-1} \tag{6.15}$$

The work presented here will deal only with the ordinary least squares estimation procedure because the main purpose is to show how sensitivity coefficients can be used to perform a model sensitivity analysis. From this section we can see that sensitivity coefficients clearly play a central role in any common estimation technique. Therefore, the procedures discussed in this work for the least squares case can be generalized for more sophisticated estimation techniques.

7. USING SENSITIVITY COEFFICIENTS TO ESTIMATE CONFIDENCE INTERVALS

In the following sections we shall briefly indicate how confidence intervals can be estimated for both the estimated parameters and the calculated heads.

7.1 Confidence Intervals And Regions For Estimated Parameters

With the statistical assumptions invoked in section 6.1, it can be shown that the quantity $(P_k - \rho_k)/P_{kk}^{1/2}$ is described by a t(m-p) distribution. P_k is the parameter value estimated by least squares, ρ_k is the correct value, P_{kk} (the square of the estimated standard error of P_k) is the diagonal element from Eq. (6.8), and m-p is the number of degrees of freedom used in calculating s^2 in Eq. (6.10). The 100(1-α)% confidence interval is approximated by [Beck and Arnold (1)]

$$\delta P_k = \pm P_{kk}^{1/2}\, t_{1-\alpha/2}\,(m-p). \tag{7.1}$$

When σ^2 is estimated by s^2, as in Eq. (6.10), the approximate boundary of the 100(1-α)% confidence region is an hyperellipsoid given by [Beck and Arnold (1)]

$$(\underline{P} - \underline{\rho})^{+}\underset{\sim}{U}^{+}\underset{\sim}{U}(\underline{P} - \underline{\rho}) = r^2 \tag{7.2a}$$

$$\delta\underline{P}^{+}\underset{\sim}{U}^{+}\underset{\sim}{U}\delta\underline{P} = ps^2 F_{1-\alpha}(p,m-p). \tag{7.2b}$$

r^2 has an F-distribution with the two degrees of freedom p and m-p, if σ is unknown. $r^2 = \sigma^2 \ell^2_{1-\alpha}(p)$ if σ is known [Beck and Arnold (1), page 294].

7.2 Confidence Intervals for Calculated Head

For the least squares case, with the assumptions of section 6.1, the covariance matrix for the calculated heads ($\underline{h}_c$) is [Beck and Arnold (1)]

$$\text{cov}(\underline{h}_c) = \underset{\sim}{U}\ \underset{\sim}{P}\ \underset{\sim}{U}^{+} \tag{7.3}$$

where the $\underset{\sim}{U}$ are the usual sensitivity matrices and $\underset{\sim}{P}$ is the parameter covariance matrix from Eq. (6.8). The diagonal elements of Eq. (7.3) give the variance of the calculated head. The square root of these diagonal elements gives the estimated standard error in calculated head.

8. MODEL DESIGN FOR MAXIMUM SENSITIVITY

In this section, a few general observations will be made regarding model sensitivity. Some examples will be given to illustrate these principles.

8.1 Minimize The Estimated Errors Or Confidence Intervals

If the confidence intervals or the estimated standard errors of the parameters can be made small, then the model has good sensitivity. From Eqs. (6.8) and (6.9), it is seen that the diagonal elements of $(\underset{\sim}{U}^{+}\underset{\sim}{U})^{-1}$ are critical in this regard. Therefore, striving to maximize the model sensitivity is equivalent to minimizing the diagonal elements of $(\underset{\sim}{U}^{+}\underset{\sim}{U})^{-1}$. The inverse of the matrix is given by its adjoint divided by its determinant.

$$(\underset{\sim}{U}^{+}\underset{\sim}{U})^{-1} = \text{adj}(\underset{\sim}{U}^{+}\underset{\sim}{U})/\left|\underset{\sim}{U}^{+}\underset{\sim}{U}\right| \tag{8.1}$$

One approach to achieve maximum sensitivity is to try to increase the determinant $\left|\underset{\sim}{U}^{+}\underset{\sim}{U}\right|$ [Beck and Arnold (1)]. However, the determinant can be increased by a simple scaling of $\underset{\sim}{U}^{+}\underset{\sim}{U}$ which does nothing for the accuracy. So one must be careful to increase $\left|\underset{\sim}{U}^{+}\underset{\sim}{U}\right|$ in such a way that the accuracy actually increases.

From Eq. (8.1), $\underset{\sim}{U}^{+}\underset{\sim}{U}$ clearly should not be singular ($|\underset{\sim}{U}^{+}\underset{\sim}{U}| \neq 0$). This means that the sensitivity coefficients and the parameters must be independent. For example, consider the case of two parameters, T and S. The least squares matrix is

$$(\underset{\sim}{U}^{+}\underset{\sim}{U}) = \begin{bmatrix} \sum_{i,n} (U^{n}_{Ti})^{2} & \sum_{i,n} U^{n}_{Ti} U^{n}_{Si} \\ \sum_{i,n} U^{n}_{Ti} U^{n}_{Si} & \sum_{i,n} (U^{n}_{Si})^{2} \end{bmatrix} ; \tag{8.2}$$

i and n denote spatial and temporal measurement locations. If U_T and U_S happen to be dependent as in Eq. (2.27), showing that $|\underset{\sim}{U}^{+}\underset{\sim}{U}| = 0$ is not difficult. Clearly, none of the sensitivity coefficients may be dependent. However, problems may arise when two or more of the sensitivity coefficients are nearly dependent. Sometimes this condition can be seen by plotting and comparing sensitivity coefficients. Another way to examine dependence between sensitivity coefficients is to calculate the sensitivity correlation matrix, an element of which has the form

$$(sr)_{ik} = (\underset{\sim}{U}^{+}\underset{\sim}{U})_{ik} / [(\underset{\sim}{U}^{+}\underset{\sim}{U})_{ii} (\underset{\sim}{U}^{+}\underset{\sim}{U})_{kk}]^{1/2}. \tag{8.3}$$

If any off-diagonal elements are in the range of .9 or greater, significant correlation exists between those sensitivity coefficients, which may result in a smaller value for $|\underset{\sim}{U}^{+}\underset{\sim}{U}|$ and problems in finding an accurate inverse.

After an inverse, $(\underset{\sim}{U}^{+}\underset{\sim}{U})^{-1}$, has been found, it is possible to examine the dependence between the aquifer parameters by looking at the elements of the parameter correlation matrix given by Eq. (6.11). If any of the off-diagonal elements approach a value of 1, a significant correlation exits between those two parameters. This indicates that the two parameters are nearly dependent and should not both be estimated.

Another indicator of the stability of the inverse [Eq. (6.5)] is the condition number of $\underset{\sim}{U}^{+}\underset{\sim}{U}$ [Strang (17)]. The condition number indicates how errors in $\underline{R}$ or $\underset{\sim}{U}^{+}\underset{\sim}{U}$ are amplified in the final solution for $\underline{\Delta P}$. Ideally, if the condition number is one, no amplification occurs. If the condition number is large, small changes in $\underline{R}$ or $\underset{\sim}{U}^{+}\underset{\sim}{U}$ might produce large changes in the solution $\underline{\Delta P}$. One might suspect that as $|\underset{\sim}{U}^{+}\underset{\sim}{U}|$ approaches zero, the condition number would grow. Thus, the condition number should be an

indicator of the dependence or near dependence of sensitivity coefficients or parameters. In the work that follows, the reciprocal condition number will usually be examined rather than the condition number. If the reciprocal condition number is near one, the matrix is well conditioned and errors are not amplified. On the other hand, if the reciprocal condition number is very small, the matrix is ill-conditioned. If the reciprocal condition number is 10^{-k} and k approaches the number of significant digits used by the computer, the matrix is said to be nearly singular at that working precision [Dongarra et al. (5)].

In many cases where the aquifer parameters vary considerably in magnitude over the model, it is helpful for accuracy and convergence to use normalized sensitivity coefficients (PU_p) and solve for relative changes in the parameters ($\Delta P/P$). Eqs. (6.3) to (6.7) can be written for these changes with minor modifications. First, define the normalized sensitivity coefficients as

$$U'^{n}_{i;k} = P_k U^{n}_{i;k} \tag{8.4}$$

and the relative parameter changes as

$$\Delta P'_k = \Delta P_k / P_k . \tag{8.5}$$

As in section 6.1, let $\sum_{n} U'^{n}_{i;k}$ be one element of the matrix $\underset{\sim}{U}'$. The normalized least squares equations can now be written as

$$(\underset{\sim}{U}'^{+}\underset{\sim}{U}')\underline{\Delta P}' = \underline{R}' \tag{8.6}$$

where one element of $\underline{R}'$ is

$$R'_k = P_k R_k . \tag{8.7}$$

As will be seen later, it is much easier visually to compare normalized sensitivity coefficients and relative parameter changes.

Earlier sections have dealt with methods for determining sensitivity coefficients. Several examples of sensitivity coefficients have been given for various models. Clearly from that work, the sensitivity functions may vary in magnitude considerably over space and time. Obviously better sensitivity will result if the measurement points in space and time, which go into the matrix $\underset{\sim}{U}$, are

chosen to primarily sample the regions where the sensitivity coefficients have their largest values. On the other hand, if the measurement points cannot be adjusted, clearly the estimated parameters will have greater uncertainty when using data from areas of low sensitivity. As a simple example of this principle, consider the sensitivity with respect to storativity for the leaky aquifer shown in Figure 9. If we have a choice, larger sensitivities clearly result when the observation well is closer to the pumped well. For an observation well at 1000 feet, head measurements taken before .01 day or after 1.0 day will contribute little to defining the storativity parameter.

In dealing with the ground-water inverse problem, we work with a set of head measurements. In many cases, more than one model specification is consistent with this head data. Other geohydrologic information may further restrict the suite of possible models. However, usually considerable latitude exists in specifying the model. In this case one should choose the model that has the greatest sensitivity to the aquifer parameters. In particular, consider the effect of boundary conditions. From earlier discussion, Eqs. (3.26) and (3.27), it was concluded that the sensitivity coefficients go to zero at a specified head boundary. However, this is not the case for a specified flow boundary. As an example of this, consider the sensitivity coefficients shown in Figures 15 and 21. Exactly the same head data is appropriate for both of these cases; only the boundary conditions at $y = 0$ and $y = 2{,}000$ are different. In Figure 15, $y = 0$ and $y = 2{,}000$ represent specified head boundaries, while in Figure 21 they are barrier boundaries. Clearly the model in Figure 21 has the potential for greater sensitivity. In general, specified head boundaries, with their resultant zero-sensitivity coefficients, result in smaller model sensitivity and larger parameter uncertainty.

There is, of course, a limit on the number of parameters that can be determined, which is the number of measurements made. As discussed earlier, the uncertainty of each parameter is related to the sensitivity of the model and the measurement errors. It makes no sense to try to determine a given parameter if the model sensitivity is very low. In practice, what is done many times is to assume that a number of nodes have a common parameter value. This collection of nodes is called a zone. It seems reasonable that the total sensitivity for the zone would be the sum of the individual nodal sensitivities. Actually, the preceeding statement is just the discrete analog of Eq. (2.16), where the area of integration is just the zone. From this discussion it seems reasonable that, through a proper summation of nodes into zones, it might be possible to obtain an acceptable level of sensitivity in each resulting zone.

If summing into zones occurs, the least squares Eq. (6.5) will be modified. To see how, consider the case of three zones. The

least squares matrix is

$$(\underset{\sim}{U}^{+}\underset{\sim}{U}) = \begin{bmatrix} \sum_i U_{i;1}^2 & \sum_i U_{i;1}\,U_{i;2} & \sum_i U_{i;1}\,U_{i;3} \\ \sum_i U_{i;2}\,U_{i;1} & \sum_i U_{i;2}^2 & \sum_i U_{i;2}\,U_{i;3} \\ \sum_i U_{i;3}\,U_{i;1} & \sum_i U_{i;3}\,U_{i;2} & \sum_i U_{i;3}^2 \end{bmatrix}. \tag{8.8}$$

Suppose zones 1 and 2 are to be combined into a single zone. The total sensitivity for the combined zone at node i is $(U_{i;1} + U_{i;2})$. If we sum the first and second row and the first and second column in $(\underset{\sim}{U}^{+}\underset{\sim}{U})$ we obtain

$$(\underset{\sim}{U}^{+}\underset{\sim}{U})_s = \begin{bmatrix} \sum_i (U_{i;1}+ U_{i;2})^2 & \sum_i (U_{i;1}+ U_{i;2})U_{i;3} \\ \sum_i (U_{i;1}+ U_{i;2})U_{i;3} & \sum_i U_{i;3}^2 \end{bmatrix}. \tag{8.9}$$

Similarly, if all three zones are to be combined into a single zone, the total sensitivity for the combined zone at node i is $(U_{i;1} + U_{i;2} + U_{i;3})$. By summing all the rows and columns in either Eq. (8.8) or (8.9), we obtain

$$(\underset{\sim}{U}^{+}\underset{\sim}{U})_s = \sum_i (U_{i;1} + U_{i;2} + U_{i;3})^2. \tag{8.10}$$

From the above discussion, it is clear that the least squares equation (6.5) may be collapsed to any convenient number of zones by summing the appropriate rows and columns of $\underset{\sim}{U}^{+}\underset{\sim}{U}$ and summing the appropriate elements of $\underline{\Delta P}$ and $\underline{R}$. It seems that it might be possible to collapse the number of parameter zones and to adjust the zone shapes with the above technique such that a minimum parameter sensitivity or maximum parameter error is achieved. Of course, this procedure would have to be tempered by knowledge of the geohydrology. The zone formation would have to satisfy the joint goals of increasing parameter sensitivity and being consistent with the known hydrogeology.

8.2 Examples Of Methods For Maximizing Model Sensitivity

In the following sections various examples will be given which illustrate techniques for increasing model sensitivity. The goal is

to increase model sensitivity until an acceptable level of error in the estimated parameters is achieved.

8.2.1 The Theis aquifer

For the Theis equation, the sensitivity coefficients attain their maximum magnitudes at infinite time and zero radius (Figures 2 and 3). Therefore, logically, observation wells should be located very close to the pumping well and observed for very long times [Yeh and Sun (20)]. Practically, there are some problems with this approach. The transmissivity value obtained from the pumping test is an average of the transmissivity in the region of the cone of depression. Locating too close to the pumping well restricts the region sampled. Also, perturbing influences may cause the drawdown near the well to deviate from the assumed model (for example, partial penetration and well construction). It is not possible to continue a pumping test indefinitely; usually a maximum duration is dictated by external influences (cost, manpower, equipment, etc.). Therefore, having a way to terminate the pumping test when the aquifer parameters had been determined accurately enough would be desirable.

As discussed in the previous section, maximizing $|U^+U|$ is one way to try and minimize parameter uncertainty. Figure 25 is a plot of $|U^+U|$ versus time for the Theis equation with the same parameters as used earlier to generate Figures 2-5. The observation well distance (r) is 1,000 feet. Notice that, as expected, $|U^+U|$ continues to increase with time. This was expected since U_T continues to increase with time (Figure 3) even though U_S is approximately constant after about one day (Figure 5). The non-smooth character of $|U^+U|$ at log cycle boundaries in Figure 25 is due to a different time sample rate in each log cycle of time (10 samples per log cycle). The dotted line extension at 1 day is the curve that would result if the same time sample interval (.1 day) had been used on two successive log cycles from .1 day to 10 days.

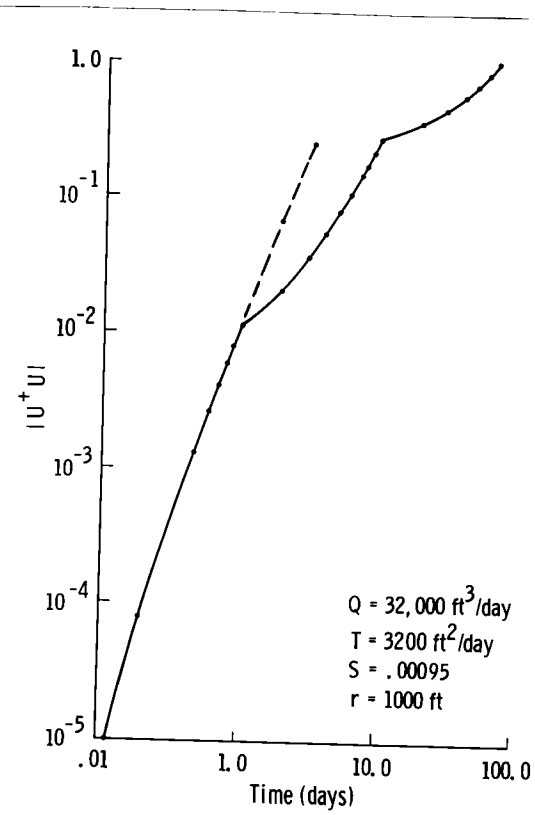

Fig. 25. $|U^+U|$ versus time for the Theis equation.

The 95% confidence intervals for transmissivity (δT) and storage (δS), as defined by Eq. (7.1), are plotted versus time in Figure 26. The head data (he) has been rounded to the nearest .1 foot and Eq. (6.10) has been used to estimate the head variance. The accuracy of T continues to increase with time. However, the curve for δS is fairly flat after about 1 day. (The confidence interval curves in Figure 26 are not monotonically decreasing because of errors in estimating σ, T, and S from the rounded data). These results might have been anticipated from the sensitivity coefficients (Figures 3 and 5). At .3 day the 95% confidence interval expressed as a percent of the parameter is 6.5% for S and 21.5% for T. At 2 days it is 3.9% for S and 3.7% for T. At 20 days it is 3.1% for S and 1.3% for T. From these results the model is seen to be more sensitive to S than to T at early times. However, as time increases, the model becomes more sensitive to T than to S.

These results suggest that sensitivity analysis could determine the duration of a pumping test needed for a given accuracy of the aquifer parameters (assuming that the Theis equation is a reasonable model). This could be done two ways. In the office before the pumping test, if one can estimate the accuracy of the head data (σ) and a range for T and S, then sensitivity analysis could predict the maximum duration needed for the desired accuracy. On the other hand, if a microcomputer can be taken to the field to record and analyse the data in real time, then sensitivity analysis would allow the computer to inform the supervisor of the current estimation accuracy and to stop the test when the desired accuracy had been reached. In this case, σ, T, and S would be estimated from the data as they are collected.

The results presented in this section have been for an observation well at 1,000 feet from the pumped well. However, the results could be used for any r value by simply scaling the time such that r^2/t remains constant. For example, at r = 100 feet, the accuracy of 3.1% for S and 1.3% for T occurs at .2 days.

8.2.2 The leaky aquifer

The leaky sensitivity coefficients are somewhat different from the Theis case (Figures 6-11). However, they still have their maximum value for small r. The time dependence shows some new features. There are three sensitivity coefficients with respect to the three parameters: transmissivity, storage, and leakage. Remember from Figure 9 that U_S has a maximum value at some time and then decreases to zero as the time increases. The other two (U_T and U_L from Figures 7 and 11) reach their maximum values and are constant after some time. For data of a certain accuracy, one might expect the accuracy of S to be constant after some time.

The 95% confidence intervals for the three parameters, as defined by Eq. (7.1), are plotted versus time in Figure 27. However, instead of plotting δP as for the Theis equation, $\delta P/P$ as a percent has been plotted; this procedure gives a much better comparison of relative sensitivities. The head data (he) has been rounded to the nearest .1 foot and Eq. (6.10) has been used to estimate the head variance. After about one day, the 95% confidence interval for S is about 5.5%. The confidence intervals of T and L continue to decrease, but at a fairly slow rate after one day. This is to be expected since $|U^{+}U|$ continues to increase slowly because U_T and U_L are nearly constant. At the end of 10 days, the confidence intervals for S, T, and L are 5.5%, 12.5%, and 16.7%, respectively. From Figure 27 we can see that the model is most sensitive to S and least sensitive to L, with the sensitivity to T falling between these two.

In the above discussion plotting $\delta P/P$ rather than just δP was more convenient. In the same way, it is easier to compare sensitivity coefficients if PU_P is plotted rather than U_P. The position of the maximum and the areas of zero values or constant values can be determined from either. For example, in Figure 9 the drawdown data for times from .01 to 1.0 days clearly is the most critical for determining the storage coefficient. However, to see relative sensitivity at a glance, it is much better to look at PU_P.

Comparing Figures 7 and 11, one might guess that a high correlation exists between T and L since the sensitivity coefficients look so similar. The correlation matrix, calculated from Eq. (6.11) for the data set of this section, bears this out. The correlation

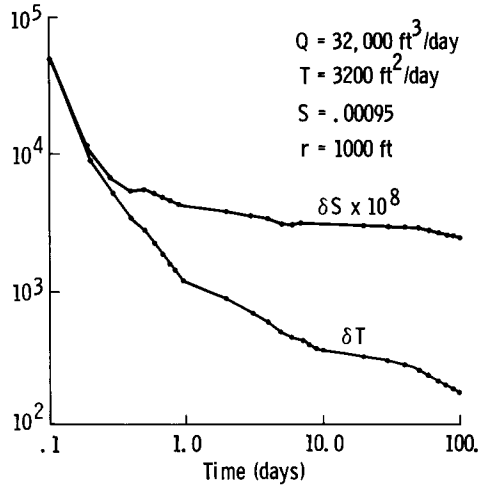

Fig. 26. 95% confidence intervals for the Theis equation, data rounded to nearest .1 ft.

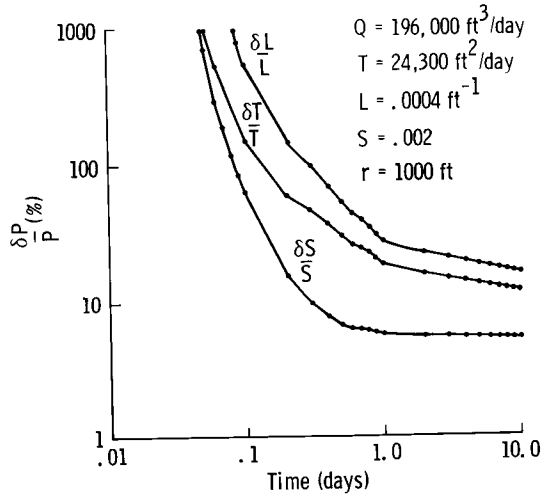

Fig. 27. 95% confidence intervals for the leaky aquifer, data rounded to nearest .1 ft.

ends, the reciprocal condition number is $.320 \times 10^{-8}$. This indicates that the matrix U^+U is nearly singular in single precision arithmetic on most computers. The estimated standard errors range from $.2 \times 10^5$ for $T_{1/2}$ to $.2 \times 10^6$ for $T_{9+1/2}$. In other words, no meaningful estimates can be made. From Eqs. (5.5) and 5.6), we know the model is insensitive to T when T is constant. Eq. (5.10) and Figure 20 indicate that the sensitivity coefficients are not zero if T varies in space. The values of T vary by an order of magnitude across this model; however, the results indicate very low sensitivity. This is a direct result of the boundary conditions chosen.

The parameter correlation matrix calculated from Eq. (6.11) for these two models is revealing. When Q is specified, the transmissivities are only related to their nearest neighbors. The parameter correlation matrix has the structure

$$\underset{\sim}{P} = \begin{bmatrix} 1 & -.5 & & & & \\ -.5 & 1 & -.5 & & 0 & \\ & \ddots & \ddots & \ddots & & \\ & & \ddots & \ddots & \ddots & \\ & 0 & & -.5 & 1 & -.707 \\ & & & & -.707 & 1 \end{bmatrix}. \qquad (8.11)$$

On the other hand, when the head is specified at both ends, all the transmissivities are highly correlated. All the entries in the parameter correlation matrix are nearly one (for example .9999). If instead of solving the 10 x 10 matrix of U^+U for all ΔT's, the first nine rows and columns of U^+U are used, the system is much better behaved. In this case, the estimated standard errors and the condition number are larger, but comparable to those found when Q is specified. This amounts to requiring $\Delta T_{9+1/2}$ to be zero, indicating the initial guess is known to be very good. The better results should not be too surprising since a known T value would allow Q to be specified. However, the parameter correlation matrix for the 9 x 9 case still shows significant correlation between several of the T's (at the .8-.9 level). All of this points out the importance of being able to specify Q in the model.

As discussed in section 8.1 resulting in Eq. (8.6), it may be helpful to use normalized sensitivity coefficients (PU_p) and solve for relative changes in the parameters, $\Delta P/P$. For the model with Q specified at one end and head specified at the other, the reciprocal condition number improved from $.362 \times 10^{-4}$ to $.161 \times 10^{-2}$ simply by using the normalized version of the least squares equations. The estimated standard errors and the parameter correlation matrix were not significantly affected since the input head values were given accurately enough already. However, the improved condition number means that the effect of errors in head would not be amplified as

matrix element for T and L is -.995. This implies that it will be difficult to obtain good estimates for both T and L with poorer quality data. Figures 6 and 10 indicate that U_T and U_L differ considerably in their radial dependences. This suggests that if more observation well data at various radii is available, the correlation between T and L would be reduced and better estimates could be made. This has been verified by numerical experiment. Adding observation wells at 100 feet and 500 feet reduces the correlation between T and L to -.80. At the same time, the 95% confidence intervals for S, T, and L reduce to 2.1%, .7%, and 2.3%, respectively, at the end of one day of pumping.

As for the Theis case, one could make a decision before the pumping test or in real time as to the duration needed for a given parameter accuracy. Of course, one must be able to give a range of aquifer parameters and data accuracy or estimate them in real time to perform this kind of sensitivity analysis. This example has pointed out that sampling in the spatial domain also affects the sensitivity. Therefore, one can choose the configuration of observation wells and duration of the pumping test based on sensitivity analysis to give the desired accuracy of the aquifer parameters. All of this assumes the leaky model is an adequate representation of the real world aquifer. In many cases, this may not be true.

8.2.3 One-dimensional steady-state model with spatially varying transmissivity

In sections 4.3 and 5.2, analytical expressions for the sensitivity coefficients were derived for two different sets of boundary conditions for the simple model described by Eq. (4.2) and Figure 12. The sensitivity coefficients, for Q specified at one boundary and head at the other, are shown in Figure 13. Some of the coefficients, for head specified at both boundaries, are shown in Figure 20. As remarked earlier, they are very different in character. At this point, we would like to know if one formulation of the problem is better than another for estimating the transmissivity distribution.

To make this judgement, we will look at three things: the condition number of U^+U, the estimated standard error, and the parameter correlation matrix. When Q is specified, the reciprocal condition number is $.362 \times 10^{-4}$ and the estimated standard error in transmissivity (see Figure 29) increases smoothly from about 35 for $T_{1/2}$ to 2,500 for $T_{9+1/2}$ (about 3.5% to 25%). The results for the standard error were obtained from Eq. (6.9), assuming $\sigma = .025$, which roughly corresponds to the head data being accurate to the nearest .1. As expected and predicted by Eq. (4.15), the model is less sensitive in areas having a larger transmissivity. However, the estimated errors seem reasonable and the inverse is well defined. On the other hand, when the head is specified at both

much during the inverse process to find the ΔT's. This should be a great advantage in a real-world situation.

At this point we would like to consider the structure of the parameter variance for this model. From Eq. (4.15) and Figure 13, we see that if $T_{k+1/2}$ is a constant for all k, then all the $U_{Ti;k}$ have the same nonzero region as in Figure 13, but they all have the same amplitude. This leads to the following structure for U^+U.

$$\underset{\sim}{U}^+\underset{\sim}{U} = \left[\frac{Q\Delta x}{\ell T^2}\right]^2 \cdot \begin{bmatrix} 1 & 1 & 1 & 1 & 1 \\ 1 & 2 & 2 & 2 & 2 \\ 1 & 2 & 3 & 3 & 3 \\ 1 & 2 & 3 & 4 & 4 \\ 1 & 2 & 3 & 4 & 5 \end{bmatrix} \tag{8.12}$$

To conserve space, the matrix is shown for only five transmissivities; the extension for any number is obvious. The inverse of this matrix is

$$(\underset{\sim}{U}^+\underset{\sim}{U})^{-1} = \left[\frac{\ell T^2}{Q\Delta x}\right]^2 \cdot \begin{bmatrix} 2 & -1 & 0 & 0 & 0 \\ -1 & 2 & -1 & 0 & 0 \\ 0 & -1 & 2 & -1 & 0 \\ 0 & 0 & -1 & 2 & -1 \\ 0 & 0 & 0 & -1 & 1 \end{bmatrix} . \tag{8.13}$$

Again, the extension to larger matrices is obvious. We see that the estimated standard error (E.S.E.) is $\sqrt{2}\ \sigma\ell T^2/Q\Delta x$ for all except the last transmissivity and it simply has the 2 replaced by 1. This is the basic structure of the variance due to the model.

The extension of Eq. (8.12) to the case where transmissivity varies spatially is

$$\underset{\sim}{U}^+\underset{\sim}{U} = \left[\frac{Q\Delta x}{\ell}\right]^2 \cdot \begin{bmatrix} T_{1/2}^{-4} & & T_{1/2}^{-2}T_{3/2}^{-2} & & T_{1/2}^{-2}T_{5/2}^{-2} \\ T_{3/2}^{-2}T_{1/2}^{-2} & & 2T_{3/2}^{-4} & & 2T_{3/2}^{-2}T_{5/2}^{-2} \\ T_{5/2}^{-2}T_{1/2}^{-2} & & 2T_{5/2}^{-2}T_{3/2}^{-2} & & 3T_{5/2}^{-4} \end{bmatrix} . \tag{8.14}$$

For simplicity a 3 x 3 matrix has been shown; the extension to any size is apparent. Likewise, the inverse is the extension of Eq. (8.13).

$$(\underset{\sim}{U}^{+}\underset{\sim}{U})^{-1} = \left[\frac{\ell}{Q\Delta x}\right]^{2} \cdot \begin{bmatrix} 2T_{1/2}^{4} & -T_{1/2}^{2} & T_{3/2}^{2} & 0 & \\ -T_{3/2}^{2} & T_{1/2}^{2} & 2T_{3/2}^{4} & -T_{3/2}^{2} & T_{5/2}^{2} \\ 0 & -T_{5/2}^{2} & T_{3/2}^{2} & T_{5/2}^{4} & \end{bmatrix} . \qquad (8.15)$$

We can see from the extension of Eq. (8.15) to an N x N matrix that

$$\text{E.S.E. of } T_{k+1/2} = \frac{\ell T_{k+1/2}^{2}}{Q\Delta x}\,\sigma \begin{cases} \sqrt{2} & 0 \leq k < N \\ 1 & k = N \end{cases} . \qquad (8.16)$$

The factor out front is the contribution to the standard error due to the transmissivity distribution; while the remaining factor is due to the model structure. This shows very clearly that the error will be greater in areas of large T since the model is less sensitive there.

The parameter variance structure and standard error estimates given in the last paragraph are actually much more important than might be supposed. The sensitivity coefficients along a streamline in a two-dimensional model are given by [McElwee (14)]

$$U_{Ti;k} = \begin{cases} -\dfrac{Q_{k+1/2}\ \Delta x_{k+1/2}}{\ell_{k+1/2}\ T_{k+1/2}^{2}} & k > i \\ 0 & \text{otherwise} \end{cases} \qquad (8.17)$$

where $Q_{k+1/2}$ is the flux of water in the streamtube between nodes k and k + 1, $\ell_{k+1/2}$ is the streamline width at that point, and $\Delta x_{k+1/2}$ is the node spacing between k and k + 1 along the streamtube. We see that this is just a straightforward extension of Eq. (4.15). Therefore, the estimated standard error of transmissivity determined along a streamline for a two-dimensional model is just the extension of Eq. (8.16) with the subscript k+1/2 attached to Q, Δx, and ℓ.

As an example of how Eq. (7.2) is used to calculate a confidence region, consider the 2 x 2 versions of Eqs. (8.12) and (8.13)

$$\underset{\sim}{U}^{+}\underset{\sim}{U} = C^{2} \begin{bmatrix} 1 & 1 \\ 1 & 2 \end{bmatrix} \qquad (8.18)$$

$$\text{where } C^2 = \left[\frac{Q\Delta x}{\ell T^2}\right]^2 \tag{8.19}$$

$$(\underset{\sim}{U}^+\underset{\sim}{U})^{-1} = C^{-2}\begin{bmatrix} 2 & -1 \\ -1 & 1 \end{bmatrix} \tag{8.20}$$

The estimated standard error is $\sqrt{2}\ \sigma/C$ for T_1 and σ/C for T_2. The matrix in Eq. (8.18) may be diagonalized by finding its eigenvalues and eigenvectors. The eigenvectors can be used to form a transformation matrix that will diagonalize Eq. (8.18) and transform to a new set of transmissivities, T_1' and T_2'. The transformed least squares matrix is

$$(U^+U)' = C^2\begin{bmatrix} \frac{3+\sqrt{5}}{2} & 0 \\ 0 & \frac{3-\sqrt{5}}{2} \end{bmatrix} \tag{8.21}$$

and the new transmissivities are

$$\Delta T_1' = \cos\Theta\ \Delta T_1 + \sin\Theta\ \Delta T_2 \tag{8.22a}$$

$$\Delta T_1' = -\sin\Theta\ \Delta T_1 + \cos\Theta\ \Delta T_2, \tag{8.22b}$$

$$\Theta = 58.3^0.$$

The above equations are those for a simple axis rotation of angle Θ. The inverse of Eq. (8.21) is easily found to be

$$(\underset{\sim}{U}^+\underset{\sim}{U})'^{-1} = C^{-2}\begin{bmatrix} \frac{2}{3+\sqrt{5}} & 0 \\ 0 & \frac{2}{3-\sqrt{5}} \end{bmatrix} = C^{-2}\begin{bmatrix} .3820 & 0 \\ 0 & 2.6180 \end{bmatrix}. \tag{8.23}$$

The estimated standard error is $.6180\sigma/C$ for T'_1 and $1.6180\sigma/C$ for T'_2.

The connection between the estimated standard errors in the original and transformed systems is given by Eq. (7.2) with $\ell = 1$. This corresponds to the 39% confidence limit [Beck and Arnold (1), page 294]. Eq. (7.2) defines an ellipse, the interior of which is the confidence region. Figure 28 shows this confidence region and its relationship to the original and transformed transmissivities. In the figure, σ/C has been set to one for convenience. The equation of the ellipse (for $\sigma/C = 1$) is

$$\frac{(\delta T_1')^2}{.3820} + \frac{(\delta T_2')^2}{2.6180} = 1 \ . \tag{8.24}$$

As mentioned in section 8.1, it is possible to sum nodes into zones to achieve an improved or acceptable level of sensitivity for the resulting number of parameters. For example, consider the 4 x 4 version of Eq. (8.12).

$$\underset{\sim}{U}^+\underset{\sim}{U} = \left[\frac{Q\Delta x}{\ell T^2}\right]^2 \cdot \begin{bmatrix} 1 & 1 & 1 & 1 \\ 1 & 2 & 2 & 2 \\ 1 & 2 & 3 & 3 \\ 1 & 2 & 3 & 4 \end{bmatrix} \tag{8.25}$$

Summing the third and fourth rows and columns results in

$$(\underset{\sim}{U}^+\underset{\sim}{U})_s = C^2 \begin{bmatrix} 1 & 1 & 2 \\ 1 & 2 & 4 \\ 2 & 4 & 13 \end{bmatrix} . \tag{8.26}$$

C^2 is defined in Eq. (8.19). The inverse of this matrix is

$$(\underset{\sim}{U}^+\underset{\sim}{U})_s^{-1} = C^{-2} \begin{bmatrix} 2 & -1 & 0 \\ -1 & 9/5 & -2/5 \\ 0 & -2/5 & 1/5 \end{bmatrix} . \tag{8.27}$$

It can be seen from Eq. (8.27) that the sensitivity to the T in the combined node zone has increased. From Eq. (8.27) the estimated standard error for the combined node zone is $\sigma/(\sqrt{5}\ C)$; this is to be compared to the original estimated standard errors of $\sqrt{2}\ \sigma/C$ for T_3 and σ/C for T_4. Assuming, of course, that it is acceptable to sum these two T's, the estimated standard errors are improved by factors of .45 and .32. This assumes σ does not change much.

As an example of the effect of summing nodes into zones, the simple model described by Eq. (4.2) and Figure 12 will be considered. The estimated standard error for ten zones has been discussed earlier and is shown in Figure 29 by the top curve. If pairs of nodes are summed into zones, the resultant estimated standard error for five zones is shown by the middle curve in Figure 29. In

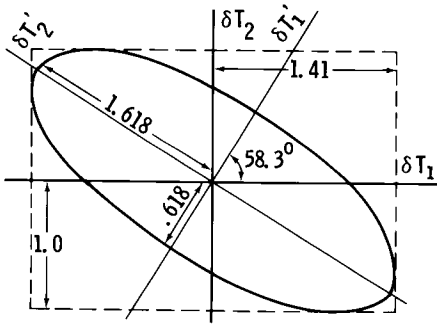

Fig. 28. 39% confidence region for the two-parameter model.

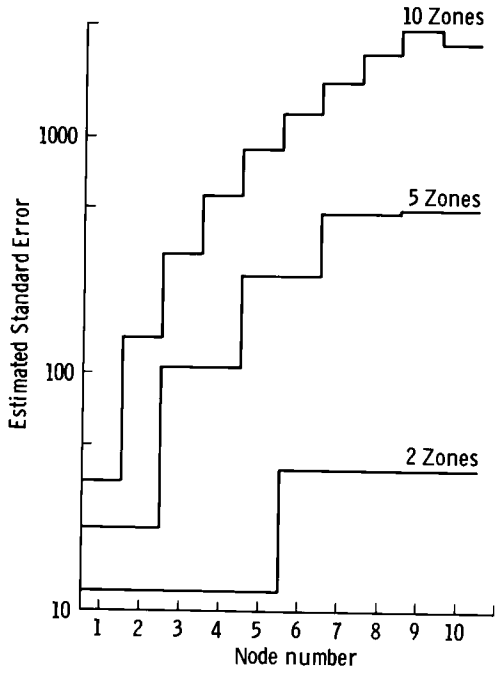

Fig. 29. Estimated standard error in transmissivity for various numbers of zones.

the extreme that five adjacent nodes are summed giving two zones, the lower curve in Figure 29 indicates the estimated standard error. Summing also improves the reciprocal condition number of the resulting least squares matrix which is solved for the parameter changes. In the ten-zone case the reciprocal condition number is .0016, while it is .0054 for five zones and .12 for two zones. Clearly, summing nodes into larger zones can be beneficial mathematically; however, this reduces the resolution of the transmissivity distribution. The maximum acceptable size of the zones would have to be determined from geohydrology considerations.

It should be noted that neither summing nor using the normalized least squares Eq. (8.6) can significantly alter an earlier conclusion: specifying the head as a boundary condition at both ends of the model leads to severe instability in the inverse process. Being able to specify Q or alternately one transmissivity value along the model has a tremendous stabilizing influence on the inverse process.

8.2.4 One-dimensional transient model with spatially varying parameters

Figure 30 shows an idealized one-dimensional transient model chosen to illustrate the use of sensitivity analysis. The model has a constant head boundary on the right (at node 11) and a barrier boundary on the left (between nodes 0 and 1). The model has a node spacing of 1,000 feet. Therefore, it is 10,500 feet between boundaries. There are 10 equations (nodes 1 to 10) to be solved for the 10 unknown head values as a function of time. The transmissivity is specified midway between node points (for example, $T_{3/2}$ occurs between nodes 1 and 2), while storativity is specified at the node points. Therefore, 10 values of transmissivity and 10 values of storativity are needed to describe this model. $T_{3/2}$ is 52,000 gpd/ft (6,952 ft^2/day) and the transmissivity increases by 2,000 gpd/ft (267 ft^2/day) as the node number increases by one. Thus, $T_{10+1/2}$ is 70,000 gpd/ft (9,358 ft^2/day). The storativity at node 1 (S_1) is .0050 and increases by .0005 as the node number increases by one. Thus, S_{10} is .0095.

The initial head distribution is assumed to be flat. The aquifer is being pumped at a rate Q equal to 1,500 gal/day (200 ft^3/day) per unit transverse length. The pumping represents a line sink located at node 7, 4,000 feet away from the constant head boundary. The model has a steady-state solution where all water being pumped comes from the constant head boundary, and the head distribution to the left of the well is flat and somewhat lower than the original level.

The correct values for the transmissivity at the 10 intermediate node points and for the storativity at the 10 node points are shown in the second column of Table 2. These values, along with the other model parameters discussed previously, were used to generate hypothetical "field" data for the hydraulic head as a function of time. These values of hydraulic head (accurate to five decimal places) were then used in an ordinary least squares inverse initial estimate for transmissivity was 61,000 gpd/ft (8,155 ft^2/day) and for storativity was .00725.

The transmissivity and storativity values calculated for early time by the inverse procedure are shown in the third column of Table 2. The early time calculations were made using hydraulic heads for 10 time steps with the total time slightly less than 2 days. For these early times the drawdown is less than 19 feet at the

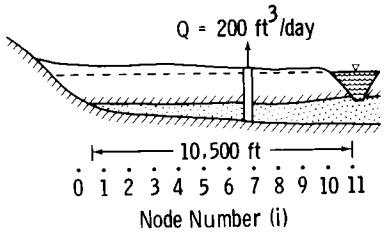

Fig. 30. A simple one-dimensional transient model [McElwee (13)].

line sink and is less than one foot farther than 3 node points away from it. The values of calculated transmissivity and storativity are within 20% of the actual values, but there is no clear evidence that the inverse procedure has been successful in finding the spatial trend of increasing T and S. At early time periods the drawdown is small and the model is fairly insensitive to the transmissivity and storativity. This insensitivity can be seen very easily by examining the sensitivity coefficients or by calculating the estimated standard error. Without a sensitivity analysis one might have expected better answers, since the head is given so accurately.

At middle times (column 4 of Table 2), when the drawdown is substantial and hydraulic heads are changing fairly rapidly with time, the greatest sensitivity and best inverse solution results. The middle time inverse calculations were made using hydraulic heads for 10 time steps between 2 days and 112 days. The system rapidly approaches steady-state for times greater than 112 days. The largest error in transmissivity is less than 7% and most values are very close to the correct values. The storativity calculations have less than 10% error and most are very close to the correct values. The largest errors occur near node 1. The reason for this will be discussed later. These results were obtained using head data accurate to 5 decimal places and a Gauss-Seidel Iterative (GSI) solution to Eq. (6.5). Using this solution routine, it was not possible to lower the error in aquifer parameters below 7-10% near node 1. However, additional work using a high-efficiency matrix package (HEMP) direct solution technique showed that the error in T and S could be made very small by using head data accurate to 5 decimal places. However, the largest of the small errors (.001%) still occurred near node 1. The reciprocal condition number of the least squares matrix for this middle time data is $.33 \times 10^{-6}$. This is much smaller than one would like and indicates that doing the matrix inversion in single precision arithmetic may lead to problems if not done efficiently. Apparently this is why the HEMP solution could achieve better accuracy. A plot of the estimated standard error ($\delta P/P$) calculated by a sensitivity analysis is shown in Figure 31. Notice that the HEMP solution near node 1 is consistent with Figure 31. However, the middle time errors in Table 2 near node 1 are much bigger than predicted by Figure 31, presumably caused by the inefficiency of the GSI solution.

The last column in Table 2 shows the transmissivity calculations as the model approaches steady-state. The storativity calculations have become unstable and cannot be made because of low sensitivity. The late time inverse calculations have been made using hydraulic heads from 5 time steps between 112 days and 850 days. The transmissivity calculations for the last 4 node points are very good. However, the calculated transmissivities for the first 6 node points are fairly bad. This can be explained by look-

ing at the sensitivity coefficients of the estimated standard errors. The sensitivity at the last 4 nodes is about 3 or 4 orders of magnitude greater than for the first 6 nodes. This lack of sensitivity is because $\partial h/\partial x$ is practically zero for the first 6 node points for times greater than 112 days.

Table 2. Inverse Calculations Over Various Time Periods (Head Data Accurate to 5 Decimal Places) [McElwee (13)]

Grid Number	Correct Value	Early Time	Middle Time	Late Time
		TRANSMISSIVITY (gpd/ft)		
1 + 1/2	52,000	59,575	48,415	72,213
2 + 1/2	54,000	62,107	55,064	69,827
3 + 1/2	56,000	64,365	55,980	71,049
4 + 1/2	58,000	66,684	57,955	70,520
5 + 1/2	60,000	69,070	60,000	71,130
6 + 1/2	62,000	71,283	62,002	243,374
7 + 1/2	64,000	55,152	64,001	64,006
8 + 1/2	66,000	56,931	66,000	65,998
9 + 1/2	68,000	58,603	68,000	67,998
10 + 1/2	70,000	60,330	70,000	69,998
		STORATIVITY		
1	.0050	.0057	.004656	Unstable
2	.0055	.0063	.006037	Unstable
3	.0060	.0069	.005801	Unstable
4	.0065	.0075	.006491	Unstable
5	.0070	.0081	.007015	Unstable
6	.0075	.0086	.007501	Unstable
7	.0080	.0080	.007998	Unstable
8	.0085	.0073	.008501	Unstable
9	.0090	.0078	.009000	Unstable
10	.0095	.0080	.009500	Unstable

Notice that for the middle time calculations shown in Table 2, the largest error in transmissivity occurs at node 1 and decreases considerably at higher numbered nodes. This should mean that the model is least sensitivity to T at node 1. A look at the sensitivity coefficients or the estimated standard should verify this. The solid curves in Figure 31 represent the estimated standard errors ($\delta P/P$) for the transmissivity and storativity at each node for $\sigma = .25 \times 10^{-5}$ (values for other σ's may be determined by the appropriate factor). The largest errors in both T and S occur at the lower numbered nodes. This is a little surprising because the sensitivity coefficients for S do not have their lowest value at

node 1 but at node 10 [McElwee (13)] near the constant head boundary. Also, notice that both solid curves in Figure 31 have practically the same $\delta P/P$ for node 1. One might suspect that T_1 and S_1 are not both independent parameters in this model. The element in the parameter correlation matrix (6.11) corresponding to T_1 and S_1 is .9917, which verifies the suspicion. Thus, the larger error in S at the lower node numbers is due to a dependence between T and S and not specifically due to low sensitivity values there.

The dashed curves in Figure 31 result when ΔT_1 is dropped from the matrix equations (6.5). This means that T_1 is assumed known and solve for S_1. Notice that the estimated standard error in S_1 drops by almost an order of magnitude. The condition number of the least squares matrix is also improved by a factor of about 6 when ΔT_1 is dropped from consideration. Eq. (2.27) suggests that maybe the model is only sensitive to the ratio of S_1/T_1. Taking values of T_1 and S_1 from Table 2, we can see that $.005/52000 \simeq .004656/48415$. Thus, a basic nonuniqueness exists near node 1. The sensitivity to transmissivity is low near node 1, which causes substantial error in the calculation of T_1. Since S_1 is dependent upon T_1, there is substantial error in S_1 also even though the sensitivity coefficients for S_1 are not particularly low near node 1.

8.2.5 Two-dimensional steady-state models

The simple two-dimensional model of section 4.4 is considered here with various boundary conditions. There are three different cases. Case 1 is defined in section 4.4 and the sensitivity coefficients are shown in Figures 15 and 16. The head is specified on three sides and the sensitivity coefficients go to zero on these boundaries. The flux is specified at x = 0. Cases 2 and 3 are defined in section 5.3.

Case 2 changes the boundary condition at y = 0 and y = 2,000 to a barrier boundary. These sensitivity coefficients are shown in Figures 21 and 22. Notice that the coefficients do not go to zero at y = 0 and y = 2,000. Since they are nonzero over a larger area than case 1, one might expect the estimated standard error to be smaller for case 2 than case 1. It cannot be seen from Figures 15, 16, 21, and 22 because the plotting routine normalizes the maximum values; however, the sensitivity coefficients for case 2 are 3 to 4 times larger than those for case 1. This is another reason to expect the estimated standard error for case 2 to be lower.

Case 3 is defined with the same boundary conditions as case 2 except the head is specified at x = 0 instead of the flux. These sensitivity coefficients are shown in Figures 23 and 24. They have about the same maximum value as case 1. The sensitivity for zone 1 is negative, while the sensitivity for zone 2 is positive. However,

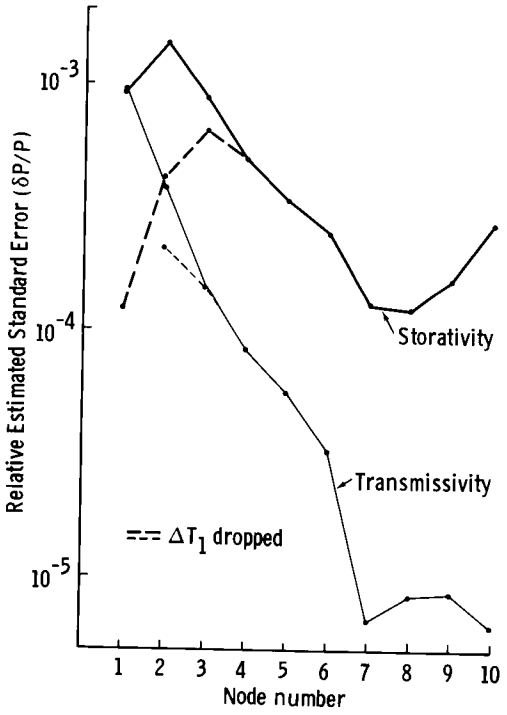

Fig. 31. Estimated standard error for one-dimensional transient model.

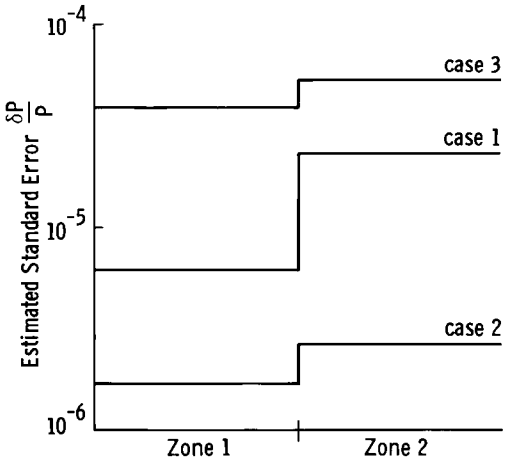

Fig. 32. Estimated standard error for the simple two-dimensional case.

except for the sign, these two sensitivity coefficients look very much alike. This is born out by the parameter correlation matrix whose off-diagonal element is .997. Therefore, the parameters T_1 and T_2 are highly correlated, and we would expect to have trouble estimating both simultaneously.

Figure 32 shows the estimated standard error for the transmissivity in the two zones for σ = .00025 (about three decimal place accuracy) for all three cases discussed above. As we expected, case 2 has the lowest error and case 3 has the highest. Case 3 has lower values of the sensitivity coefficients than case 2, and they appear to be nearly dependent. Therefore, logically case 3 should have the largest estimated standard error. Case 1 is somewhat intermediate, the sensitivity coefficients are considerably lower than case 2, but the parameters have a low correlation. With only two large zones, the zero values of the sensitivity coefficients on three boundaries for case 1 do not play a large role. However, if we had several more zones, clearly any small zone near one of the head specified boundaries would have a fairly large estimated standard error due to the low sensitivity induced by the boundary condition.

The above examples illustrate several important points, but they are not very realistic; therefore, we looked at the data and model presented by Yakowitz and Duckstein (19) for a part of the Tucson basin. The head and transmissivity maps are shown in Figures 33 and 34. The model area is shown by the smaller square in each figure. Yakowitz and Duckstein have concluded that the model is not very sensitive to the transmissivity and that the error for least squares estimation of parameters should be quite high, even for only nine zones. They do not give a detailed discussion of the boundary conditions used in their model. However, it seems clear from one sentence in their paper and the above results that they were using a head-specified boundary condition all the way around the model. From the earlier examples in this section and previous discussion in this paper, we would expect this to be the most unstable case.

We have performed a sensitivity analysis for the data and model presented by Yakowitz and Duckstein for various boundary conditions and number of zones. For a large number of zones (81), we also find the estimated standard error to be quite large for most boundary conditions. However, noticable improvement occurs when some boundary fluxes are specified. When the head is specified as a boundary condition all the way around the model, the estimated standard error is so large that no meaningful estimate can be made at all. If the model is zoned into nine zones and some fluxes specified on the boundaries, we find the estimated standard error for the zones ranges from 9.3% to 100%. Once again, if head is specified on all boundaries, no meaningful estimate can be made and high correlation is observed between parameters. If 4 transmis-

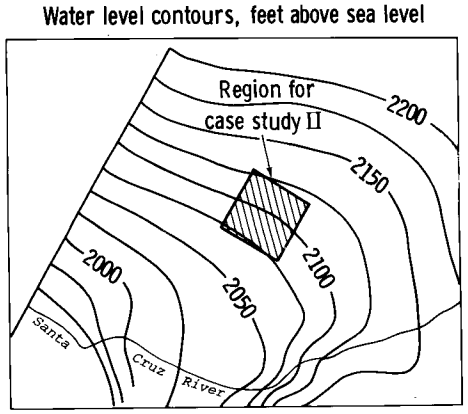

Fig. 33. Head map for the Yakowitz and Duckstein (19) model.

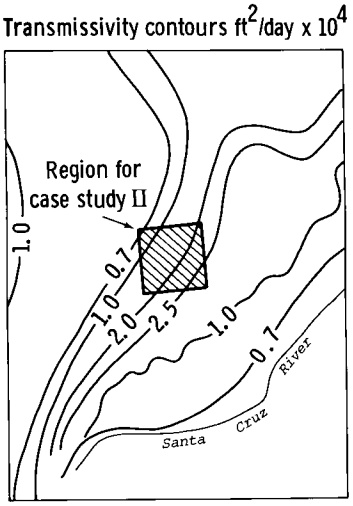

Fig. 34. Transmissivity map for the Yakowitz and Duckstein (19) model.

sivity zones are used and some boundary fluxes are given, we find the estimated standard error ranges from 4.3% to 16.9%. As before, if the head is specified all the way around, the estimated error is too large to make any meaningful estimate and the parameters show a high correlation. In all this work, the value of σ was estimated from the data and was in the range of .8 to .9 feet.

This example from a real-world situation shows clearly the advantages of using some of the techniques discussed in this paper to make the parameter-estimation procedure better conditioned. In paricular, boundary conditions are very important. The sensitivity should be made as large as possible over a large extent of the model. One must insure that the sensitivity coefficients and the parameters are not dependent. Zonation by summing nodes can be used to increase sensitivity.

9. SUMMARY AND CONCLUSIONS

This paper has given the definition of a sensitivity coefficient and shown how they may be used to perform a sensitivity analysis. A first-order sensitivity formalism has been presented to calculate the perturbed head due to a change in an aquifer parameter. We have discussed various methods of determining sensitivity coefficients and examined the effect of boundary conditions. Several examples of sensitivity coefficients have been given in some detail for a variety of models and boundary conditions. We have shown how the sensitivity coefficients enter the least squares parameter-estimation formalism and how confidence intervals and estimated standard errors can be found. We have seen that sensitivity coefficients are an essential part of parameter-estimation and that an intelligent sensitivity analysis can lead to a more stable and better conditioned inverse process.

Some general guidelines can be given for increasing the model sensitivity, leading to more accurate parameter estimation. For maximum sensitivity, the measurements of head should occur at locations and times where the sensitivity coefficients are near their maximum values. Sensitivity coefficients are greatly influenced by boundary conditions; therefore, the boundary conditions giving the largest sensitivity, consistent with the data and known hydrogeology, should be chosen. We have seen the importance of being able to specify some fluxes for the model. Emsellem and de Marsily (6) have commented on the importance of knowing some fluxes or transmissivities in the groundwater inverse problem. This requires fairly accurate knowledge of the slope of the hydraulic head and the transmissivity at some locations. Judging from the improved stability and accuracy that can be obtained, our field methods should be geared toward this goal. The sensitivity coefficients and the parameters should be independent. This can be examined by looking at plots of the sensitivity coefficients and by calculating the

sensitivity and parameter correlation matrices. Zoning by summing nodal sensitivities can lead to improved model sensitivity; however, that must be balanced with a loss of transmissivity resolution. Using these guidelines, the goal is to select a model with maximum (or at least a certain minimum) sensitivity to the aquifer parameters, based on a knowledge of sensitivity coefficients and their properties.

10. REFERENCES

1. Beck, J. V., and Arnold, K. J., *Parameter Estimation in Engineering and Science,* John Wiley and Sons, New York, N.Y., 1977.
2. Cobb, P. M., McElwee, C. D., and Butt, M. A., "Analysis of Leaky Aquifer Pumping-Test Data: An automated Numerical Solution Using Sensitivity Analysis," *Ground Water,* Vol. 20, No. 3, 1982, pp. 325-333.
3. Cooley, R. L., "A Method of Estimating Parameters and Assessing Realiability of Models of Steady State Groundwater Flow. 1. Theory and Numerical Properties," *Water Resources Research,* Vol. 13, No. 2, 1977, pp. 318-324.
4. Cooley, R. L., "A Method of Estimating Parameters and Assessing Reliability for Models of Steady State Groundwater Flow. 2. Application of Statistical Analysis," *Water Resources Research,* Vol. 15, No. 3, 1979, pp. 603-617.
5. Dongarra, J. J., Bunch, J. R., Moler, C. B., and Stewart, G. W., *Linpack Users' Guide,* 3rd ed., Society for Industrial and Applied Mathematics, Philadelphia, PA., 1979.
6. Emsellem, Y., and de Marsily, G., "An Automatic Solution for the Inverse Problem," *Water Resources Research,* Vol. 7, No. 5, 1971, pp. 1264-1283.
7. Hantush, M. S., and Jacob, C. E., "Non-Steady Radial Flow in an Infinite Leaky Aquifer," *Transactions of the American Geophysical Union,* Vol. 36, 1955, pp. 95-100.
8. Hildebrand, F. B., *Advanced Calculus for Applications,* Prentice-Hall, Englewood Cliffs, New Jersey, 1962, pp. 360.
9. Knowles, T. R., Claborn, B. J., and Wells, D. M., "A Computerized Procedure to Determine Aquifer Characteristics," *Water Resources Center Pub. No. WRC-72-5,* Texas Technological University, Lubbock, Texas, 1972.
10. Lighthill, M. J., *Introduction to Fourier Analysis and Generalized Functions,* Cambridge University Press, New York, N.Y., 1958.
11. McElwee, C. D., and Yukler, M. A., "Sensitivity of Groundwater Models With Respect to Variations in Transmissivity and Storage," *Water Resources Research,* Vol. 14, No. 3, 1978, pp. 451-459.
12. McElwee, C. D., "A One-Dimensional Study of the Groundwater Inverse Problem Using Sensitivity Analysis," *Open File Report 82-12,* Kansas Geological Survey, Lawrence, Kansas, 1982.

13. McElwee, C. D., "Sensitivity Analysis and the Ground-Water Inverse Problem," *Ground Water,* Vol. 20, No. 6, 1982, pp. 723-735.
14. McElwee, C. D., "The 2-D Inverse Problem as a Suite of 1-D Problems," *Open File Report 82-13,* Kansas Geological Survey, Lawrence, Kansas, 1982.
15. Neuman, S. P., and Yakowitz, S., "A Statistical Approach to the Inverse Problem of Aquifer Hydrology. 1. Theory," *Water Resources Research,* Vol. 15, No. 4, 1979, pp. 845-860.
16. Neuman, S. P., "A Statistical Approach to the Inverse Problem of Aquifer Hydrology. 3. Improved Solution Method and Added Perspective," *Water Resources Research,* Vol. 16, No. 2, 1980, pp. 331-346.
17. Strang, G., *Linear Algebra and Its Applications,* 2nd ed., Academic Press, Inc., New York, N.Y., 1980.
18. Theis, C. V., "The Relation Between the Lowering of the Piezometric Surface and the Rate and Duration of Discharge of a Well Using Groundwater Storage," *Transactions American Geophysical Union,* Vol. 16, 1935, pp. 519-524.
19. Yakowitz, S., and Duckstein, L., "Instability in Aquifer Identification: Theory and Case Studies," *Water Resources Research,* Vol. 16, No. 6, 1980, pp. 1045-1064.
20. Yeh, W. W.-G., and Sun, N.-Z., "An Extended Identifiability in Aquifer Parameter Identification and Optimal Pumping Test Design," *Water Resources Research,* Vol. 20, No. 12, 1984, pp. 1837-1847.

11. LIST OF SYMBOLS

A	Area of integration
B	Model boundary
C	Constant
E	Squared error function
F	Arbitrary function or statistical F distribution
H	Specified hydraulic head
K'	Permeability of semiconfining bed
L	Leakage factor for leaky aquifer
N	Total number of grid spaces for 1-D model
$\underline{P}$	Parameter vector
$\underset{\sim}{P}$	Parameter covariance matrix
Q	Water flux for a model
Q'	Water flux per unit model area
Q''	Water flux per unit length of boundary
R	Maximum x value for 1-D model, region of interest for a model, or right hand side of the least squares equation
S	Storage coefficient
T	Transmissivity

U_T	Sensitivity coefficient for transmissivity
U_S	Sensitivity coefficient for storage coefficient
$\underset{\sim}{U}$	Sensitivity matrix
$\underset{\sim}{U}'$	Normalized sensitivity matrix
$\underset{\sim}{V}$	Weight matrix for prior estimates of parameters
$\underset{\sim}{W}$	Weight matrix for head observations
f	Arbitrary function
h	Hydraulic head
h^*	Perturbed hydraulic head
h_e	Experimentally measured head
ℓ_2	Perpendicular direction in cross-sectional models
$\ell^2_{1-\alpha}$	Statistical ℓ distribution
m'	Thickness of semiconfining bed
p	Number of parameters
r	Radial distance from pumped well, or an F distribution in Eq. (7.2a).
$\underset{\sim}{r}$	Parameter correlation matrix
s	Drawdown
t	Time
$t_{1-\alpha/2}$	Statistical t distribution
u,y	Dummy variables of integration
$x,\underline{x}$	Cartesian coordinate value or vector
α	Related to confidence interval of statistical distributions
Γ	Model boundary
Δ	Change in some quantity
Δh	Change in head
ΔL	Change in leakage factor
$\underline{\Delta P}$	Vector of parameter changes
$\overline{\Delta S}$	Change in storage coefficient
ΔT	Change in transmissivity
Δx	Grid spacing
δ_{ij}	Kronecker delta
δP_k	Confidence interval for parameter P_k
$\delta(x-x_o)$	Delta function
$\theta(x-x_o)$	Heaviside function
$\rho_k,\underline{\rho}$	Correct value of P_k or parameter vector
σ	Variance of error in head
$\frac{\partial}{\partial n}$	Normal derivative
i,j,k,ℓ	Node indices, used as subscripts
m	Zone index, used as a subscript
n	Time index, used as a superscript
$'$	Used to denote normalized or transformed quantities
$\underline{\ }$	Underline indicates a vector quantity
$\sim$	Underline indicates a matrix
$+$	Superscript indicating transpose of a vector or matrix